Universitat Autònoma de Barcelona

SUPRACLAVICULAR ARTERY PERFORATOR FLAP ANATOMICAL STUDY, IMAGING FINDINGS, AND CLINICAL APPLICATIONS

HEMIN OATHMAN SHERIFF

Universitat Autònoma de Barcelona

SUPRACLAVICULAR ARTERY PERFORATOR FLAP

ANATOMICAL STUDY, IMAGING FINDINGS, AND CLINICAL APPLICATIONS

DOCTORATE THESIS

BY

HEMIN OATHMAN SHERIFF

BARCELONA 2018

Universitat Autònoma de Barcelona

SUPRACLAVICULAR ARTERY PERFORATOR FLAP

ANATOMICAL STUDY, IMAGING FINDINGS, AND CLINICAL APPLICATIONS

A THESIS

Submitted to the Department of Surgery at the University Autonoma de Barcelona in Partial fulfillment of the requirements for the Degree of

Doctorate (PhD) in Plastic Surgery

By

HEMIN OATHMAN SHERIFF

Supervisor and Thesis Director

Prof. Jaume Masia Ayala

Tutor

Prof. Xavier Rius Cornado

Barcelona 2018

Universitat Autonoma de Barcelona

Department of Surgery

Xavier Ruis Cornado PhD Jaume Masia Ayala PhD

Certified

The thesis with title *“Supraclavicular artery perforator flap, anatomical study, imaging findings and clinical applications”*, has been prepared and written by licensed author Hemin Oathman Sheriff under our directions and supervision, to be presented and defended in the tribunal in order to obtain the grade of doctorate.

Barcelona …………., de ……….. de 2018

ACKNOWLEDGMENTS

Firstly, all my praises and thanks goes to God, the merciful and the compassionate.

I am indebted to my family and friends, for their support, dedication, love and inspiring me at throughout my life.

I would like to express my sincere gratitude to my supervisor and director Dr. Jaume Masia and to my tutor Dr Xavier Ruis for their directions, suggestions and guidance which helped me to complete this project successfully.

I would like to especially thank Dra Carmen Vega, Dra Debora Bernandez, Dr Kawa Mahmood, Dr Aram Jamal, Dr Jawad Hawas, Dr Juan Clavero, Dr Nizar Hamawandi, Dra Esther Granell, Dra Shokha Kareem, and Dr Kosrat Najim for their help in data collection in this study, and I'm really grateful to all of them.

With a special mention to Dr Ignasi Gich and Dra Chro Salih for performing the statistical analysis of this project.

TABLE OF CONTENTS

LIST OF FIGURES

LIST OF TABLES

LIST OF VIDEOS

ABBREVIATIONS

3D	Three-dimension.
CT	Computed tomography.
CTA	Computed tomography angiography.
DSA	Digital Subtraction Angiography.
GA	General anesthesia.
GE	General Electric.
HHD	Handheld Doppler.
ICG	Indocyanine green.
ICGA	Indocyanine Green Fluorescent Angiograms.
MRA	Magnetic Resonance Angiogram.
PCIP	Percutaneous Coronary Intervention Procedure.
PDE	Photodynamic Eye.
SAI	supraclavicular artery island.
SCF	Supraclavicular flap.
SIF	Supraclavicular Island flap.
STCAP	Supraclavicular Flap Transverse cervical artery perforator.
TCA	Transverse Cervical Artery.
TU	Triplex ultrasound.

Chapter

1 1

Introduction and Literature Review

a

1. Introduction

1.1. General principles about the flaps

1.1.1. Definition of flaps

A flap consists of tissue that is mobilized on the basis of its vascular anatomy (1).

A skin flap consists of skin and subcutaneous tissue that are transferred from one part of the body to another with a vascular pedicle or attachment to the body being maintained for nourishment (2).

A locoregional flap should also leave a minimum of donor site morbidity and preferably be hidden beneath the clothing. Hence, the more adjacent the donor site, with better color, thickness, texture match and intact sensation offers best (3, 4).

1.1.2. History of the flap

It is not possible either to establish the exact date of the work (it is thought to have been written about 600 BC), In the *Áyurvédam*, the Indian sacred book of knowledge which deals with medicine, the missing portions of the nose were reconstructed using local flaps transposed from the cheek, Figure 1. An accurate description of blunt (*yantra*) and sharp (*sastra*) instruments necessary to perform surgical operations in general and rhinoplasty in particular is supplied (1).

Figure 1: the missing portions of the nose were reconstructed using local flaps transposed from the cheek (1).

1.1.3. Flap classification

Flaps can be classified according to: (1- **Circulation** , 2- **Composition** ,3- **Contiguity** , 4- **Contour ,** and 5- **Conditioning**) (5).

1.1.3.1. Circulation:

The circulation to flaps can be further subcategorized into:

- Random flaps have no directional blood supply and are not based on any known vessel.

- Axial flaps: contain a named artery, they are divided into (direct; fasciocutaneous; musculocutaneous; or venous).

1.1.3.2. Composition:

Flaps can be classified by their composition, as:

- Cutaneous
- Fasciocutaneous
- Fascial
- Musculocutaneous
- Muscle only
- Osseocutaneous
- Osseous.

1.1.3.3. Contiguity:

Flaps can be classified by their source, as:

- Local flaps: These are composed of tissue adjacent to the defect.
- Regional flaps: These are composed of tissue from the same region of the body as the defect.
- Distant flaps: Pedicled distant flaps are from a distant part of the body to which they remain attached.
- Free flaps: There are completely detached from the body and anastomosed to recipient vessels close to the defect.

1.1.3.4. Contour:

Flaps can be classified by the method in which they are transferred into the defect.

- Advancement: is to facilitate advancement of a flap into a defect, Figure 2. a, b,and c.
  a) V-Y advancement.
  b) Rectangular advancement.
  c) Z-plasty.
- Transposition: The flap is moved into a defect from an adjacent position must be closed by another method, Figure 3.
- Rotation: The flap is rotated into the defect, Figure 4 a and b.
- Interpolation: these flaps are moved into a defect either under or above an intervening bridge of tissue.

1.1.3.5. Conditioning (Delay):

Conditioning is any preoperative maneuver which will result in increased flap survival.

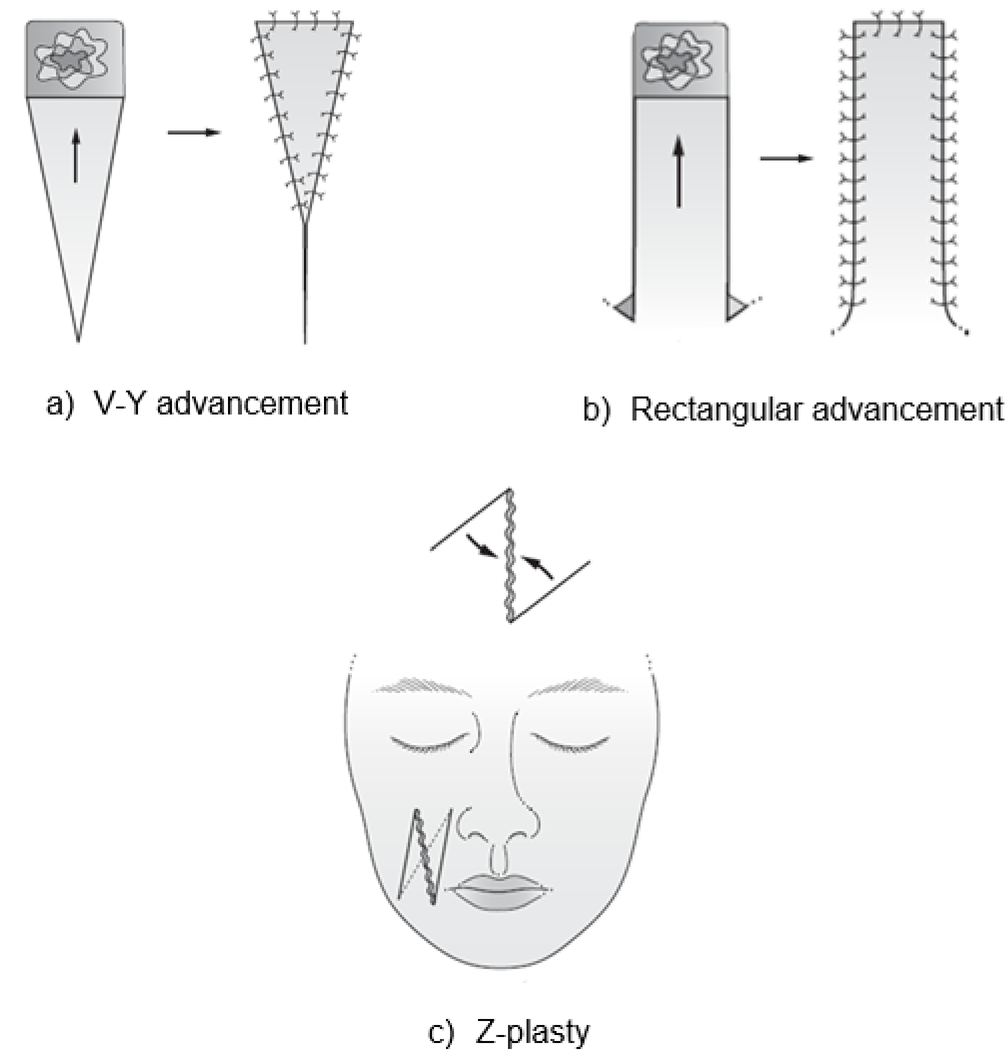

Figure 2: a - Advancement: V-Y advancement, Figure 2 b- Rectangular advancement, Figure 2 c- Z-plasty (5).

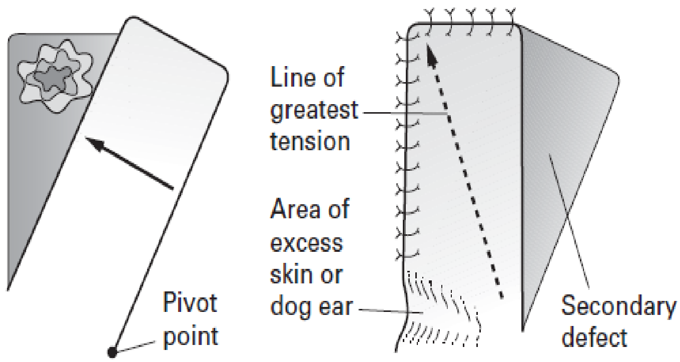

Figure 3: The Transposition flap is moved into a defect from an adjacent position (5).

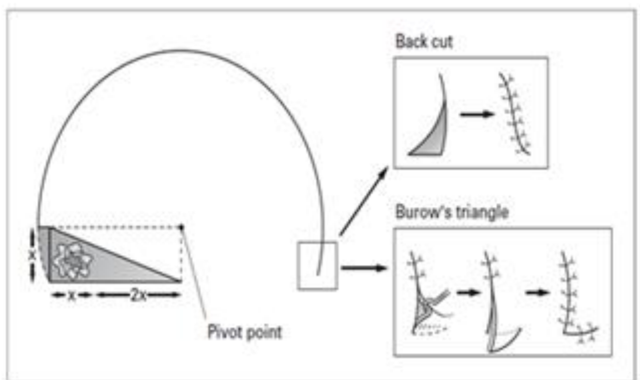

a

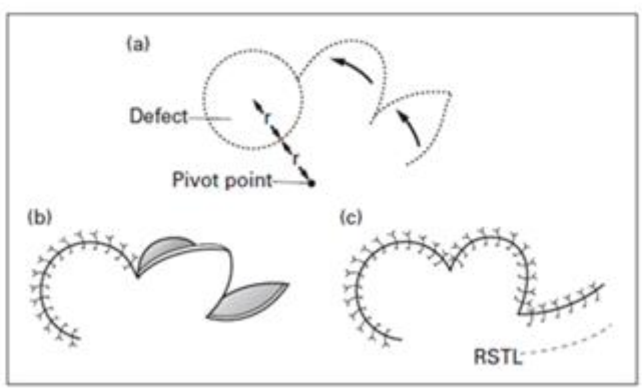

b

Figure 4 a & b: the flap is rotated into the defect (5).

1.1.4. History of imaging techniques for flap design and assessments

In 1975, Aoyagi et al first reported the use of a handheld Doppler for localization of the feeding vessels for flap design in facial reconstruction (6, 7). In the mid-1970's, angiography considered to be the gold standard, was supplanted by the use of digital subtraction angiography to determine vascular anatomy used in flap design, particularly for the lower extremities (8, 9). Use of the color Doppler scanner in flap design was later introduced in the 1980's and became a popular mapping technique in the 1990's (7, 10).

Masia et al in 2006, described the use of CT in the planning of perforator flaps in breast reconstruction (11). Around the same period, MRA was introduced to localize perforators (12). Smit et al reported the use of CTA preoperatively to reduce the time of free flaps surgery in 2009 (13). Indocyanine green and near-infrared imaging were used to identify perforators in flap design (14).

Smit et al in 2010 performed an overview of methods for vascular mapping in flap planning (7). Su et al performed a study on contrast-enhanced ultrasound in preoperative perforator flap design in 2012, that included 4 cases of mapping the perforators of the transverse cervical artery (15) .

1.2. Definition, history, and literature review of the supraclavicular artery flap

The supraclavicular artery island (SAI) flap is a local fasciocutaneous flap taken from skin on the shoulder and supraclavicular area. The supraclavicular island flap has been widely used in head and neck reconstruction, providing an alternative to traditional techniques like regional or free flaps (16).

The flap is based off an axial vessel branching from the thyrocervical trunk or transverse cervical artery. The color match, thinness, pliability, hair free skin of supraclavicular artery flap parallels that of the head and neck region and provides a superior cosmetic outcome when compared to free tissue transfer flaps from such as the forearm, abdomen, or thigh (16-18).

In the year 1842, Thomas Mutter in Philadelphia described a random flap in the shoulder region (16, 19, 20). In 1903, Toldt, an anatomist, first illustrated and named the vessel arteria cervicalis superficialis. It originates from the thyrocervical trunk exiting between the trapezius and sternocleidomastoid muscles (18).

The first clinical application of a flap from the shoulder was performed by Kazanjian and Converse in 1949 (16, 21, 22). The supraclavicular flap was first described by Lamberty in 1979 as an axial pattern fasciocutaneous flap (23).

In 1983, Lamberty and Cormack in an anatomical study on cadavers, they found a vessel cephalad to the clavicular insertion of the trapezius muscle and they named it the supraclavicular artery (24). Beginning in the 1990s, Pallua et al. “rediscovered” this flap and popularized its use by performing detailed anatomical studies examining the vascularity of what is known today as the supraclavicular island flap (25, 26). Following that Pallua et al published several clinical series of supraclavicular artery flaps for reconstruction of post-burn neck contracture, and also in oncologic head and neck reconstruction, and they found the flap safe and reliable for immediate resurfacing of the cervical defects (20, 26-28).

Di Benedetto et al. in 2005, reported this flap as reliable for covering oral tissue lining after oncologic resection (29). Chiu et al described the use of the supraclavicular artery flap for functional pharyngeal reconstruction (17, 30).

In a published study in 2017 by Kadakia et al on 63 patients, they reported the supraclavicular artery flap may be a more suitable option for patients with cutaneous defects than mucosal defects, given the reliability and lower propensity for postoperative complications (31).

Razdan et al in a recent study in 2015, reported the supraclavicular artery island flap is safe for use in patients who have had an ipsilateral neck dissection involving level IV or V lymph nodes and/or radiation treatment to the neck (32).

In the past decade, this flap has been widely used and discussed (33, 34). Anatomical studies supporting it have been performed (35-37) . The pre-expanded flap (28, 38) and bilobed flap versions have also been developed (39-41) .

The use of supraclavicular flap for head and neck reconstruction was well described in many articles (4, 17-19, 26-30, 33, 37, 38, 40, 42-54), with a special focus on the length of flaps, and their rate of necrosis (Table 2).

1.3. Nomenclature of the supraclavicular artery and supraclavicular artery flap

The vessel name 'supraclavicular artery' is based on the work of Lamberty (22-24), and has been used since then.

There are highly variable nomenclature of this flap, and named differently in different publications; Supra-clavicular axial patterned island flap (55), Transverse cervical artery (TCA) fasiocutaneous flap (56), Supraclavicular artery flap (36, 57), anterior supraclavicular artery perforator (a-SAP) flap (35) , Supraclavicular Island flap (SIF) (19), supraclavicular artery island flap (SAIF) (32), Supraclavicular flap, Transverse cervical artery perforator (STCAP) (58), Supraclavicular flap (SCF) (25, 59, 60) .

Those names developed to clarify which flap is described and to differentiate these descriptions from other flaps harvested in the supraclavicular region (35, 38).

1.4. Anatomy of the supraclavicular artery

1.4.1. Vascular tree of supraclavicular artery

1.4.1.1. Thyrocervical trunk

The thyrocervical trunk (*truncus thyreocervicalis; thyroid axis*), is a short thick trunk, which *arises* from the front of the first portion of the subclavian artery, close to the medial border of the Scalenus anterior, and divides almost immediately into three branches, the inferior thyroid, transverse scapular, and transverse cervical, (Figure 5) (61).

1.4.1.2. Transverse cervical artery

The Transverse Cervical Artery (*a. transversa colli; transversalis colli artery*), lies at a higher level than the transverse scapular; it passes transversely above the inferior belly of the Omohyoideus to the anterior margin of the Trapezius, beneath which it divides into an ascending and a descending branch. It crosses in front of the phrenic nerve and the Scaleni, and in front of or between the divisions of the brachial plexus, and is covered by the Platysma and Sternocleidomastoideus, and crossed by the Omohyoideus and Trapezius, (Figure 5) (61).

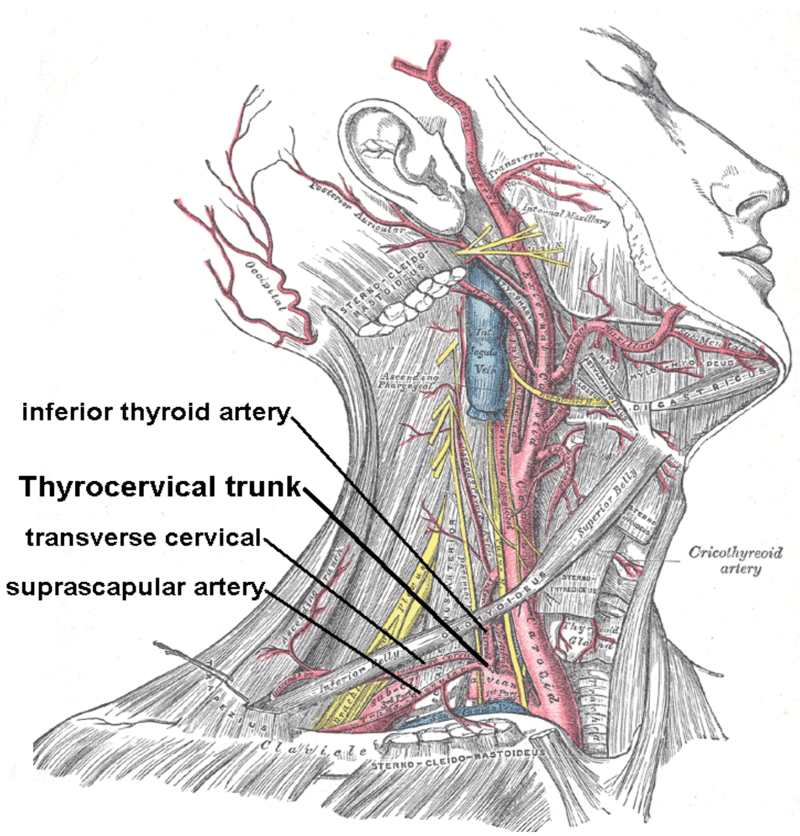

Figure 5: Thyrocervical trunk and branches (61).

1.4.1.3. Supraclavicular artery

The Transverse Cervical Artery runs posteriorly and laterally toward the trapezius muscle and travels beneath the omohyoid muscle and superficial to the scalene muscles and brachial plexus within the fibro-fatty tissue of the supraclavicular fossa. After passing underneath the omohyoid muscle, it gives off the Supraclavicular artery and perforators to the supraclavicular skin (53).

The supraclavicular pedicle emerges from transverse cervical vessel and is located in the triangle formed by the dorsal edge of the sternocleidomastoid muscle, the external jugular vein and the medial part of the clavicle, Figure 6, (30, 34, 46).

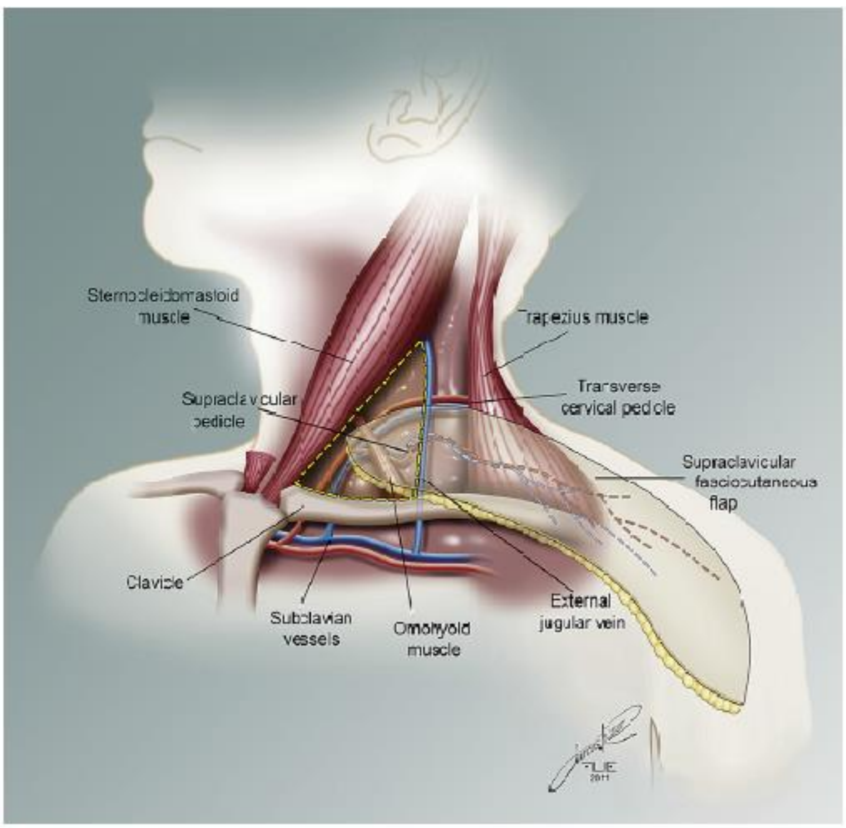

Figure 6: The supraclavicular pedicle emerges from transverse cervical vessel and is located in the triangle formed by the dorsal edge of the sternocleidomastoid muscle, the external jugular vein and the medial part of the clavicle (30).

1.4.2. Cadaver study of the supraclavicular artery

From the study by Vinh et al, used 40 flaps from both sides of 20 preserved cadavers. After designing the flaps on the shoulders of the cadavers, they identified the subclavian artery, the thyrocervical trunk, the transverse cervical artery, and its branch, the supraclavicular artery, Figure 7. They reported that the supraclavicular artery branched from the transverse cervical artery in all 40 specimens (100 percent). Although it arose from the middle third of the clavicle in 90 percent of the specimens, it arose from the lateral third of the clavicle in four specimens (10 percent) (37).

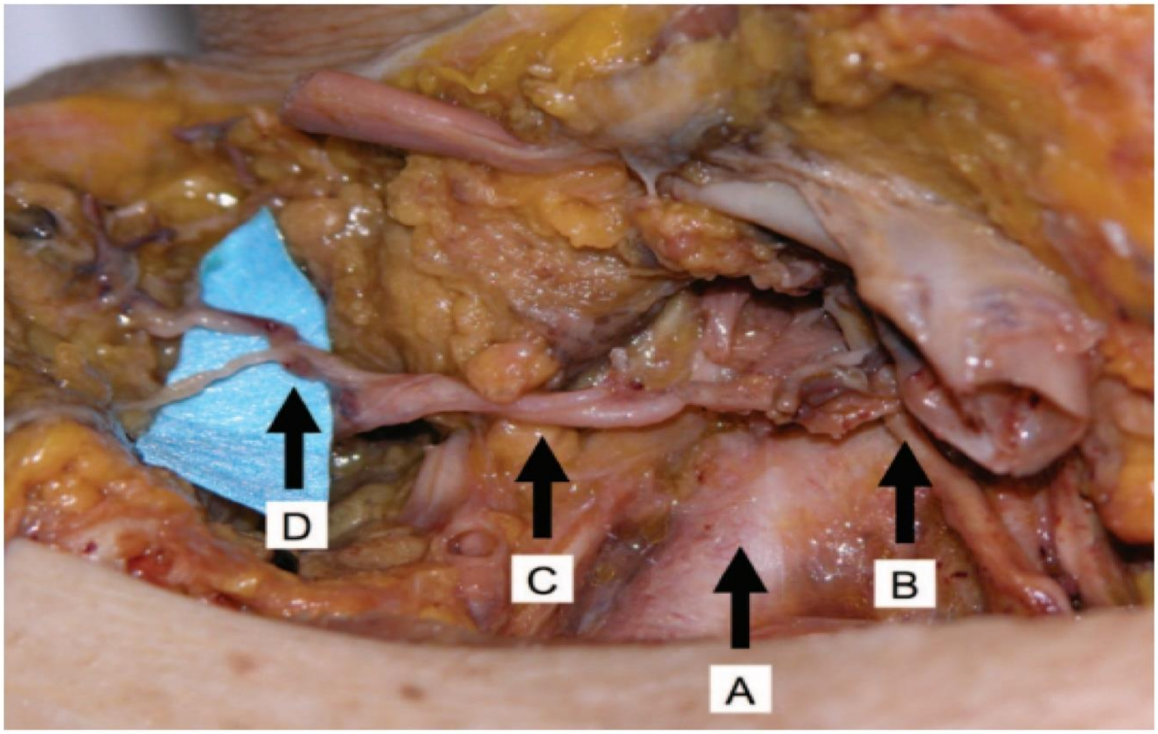

Figure 7: Cadaver dissection shows Supraclavicular vascular tree A: Subclavian artery. B: Thyrocervical trunk .C: Transverse cervical artery D: Supraclavicular artery (37).

From a research by Tayfur et al on Fourteen formalin fixed cadavers were dissected bilaterally, and 28 supraclavicular arteries were evaluated. The origin of the supraclavicular artery was transverse cervical artery in 62.9% and suprascapular artery in 37.1% of the cases. The origin of the artery was at the level of the medial third of the clavicle in 3.7%; 3.7% of the cases were at the junction of medial and middle third of the clavicle, 33.3% at the level of middle third of the clavicle, 11.1% at the junction of middle and lateral thirds, 44.4% at the level of lateral third, and 3.7% at the level of acromioclavicular joint. The mean values of the results were as follows: The diameter of the artery was 1.0 mm at the origin. The average length of the artery was 70.8 mm. In all dissections, the artery was deep to the platysma muscle (36) .

Pallua et al, in an anatomical study with 10 fresh cadavers they reported that, apart from the classical Supraclavicular branch of TCA, the anterior supraclavicular artery branch from TCA emerges from above the clavicle directly lateral to the lateral head of the sternocleidomastoid muscle, pierces the platysma, crosses the clavicle in its medial third and then runs in the direction of the deltoideo-pectoral fossa, and they claimed this vessel is constant. They reported in their clinical experience, both vessels are always present (35).

Another Anatomical study of 10 fresh cadavers by Balakrishnana et al, in which 20 transverse cervical vascular system traced up to the thyrocervical trunk. They found that in all specimens the Supraclavicular artery arises from the Thyrocervical artery as it crosses upper trunk on an average 8.5 cm from medial end of clavicle and 7.5 cm from mid-point of clavicle with 1.5 mm average diameter at its origin (4).

1.4.3. Imaging study of the supraclavicular artery

Ten supraclavicular artery island flaps were harvested from fresh cadavers. Each flap was injected with contrast media and subjected to dynamic computed tomographic scanning using a GE Light speed 16-slice scanner. Static computed tomographic scanning was also undertaken using a barium-gelatin mixture. The scan shows that the entire skin paddle was perfused in the majority (9 out of 10) of the flaps, Figure 9. Direct linking vessels and recurrent flow by means of the subdermal plexus were found to convey the flow of contrast between adjacent perforators. This explains how perfusion extends to adjacent perforators by means of interperforator flow, and how perfusion is maintained all the way to the distal periphery of the flap, Figure 8, (25).

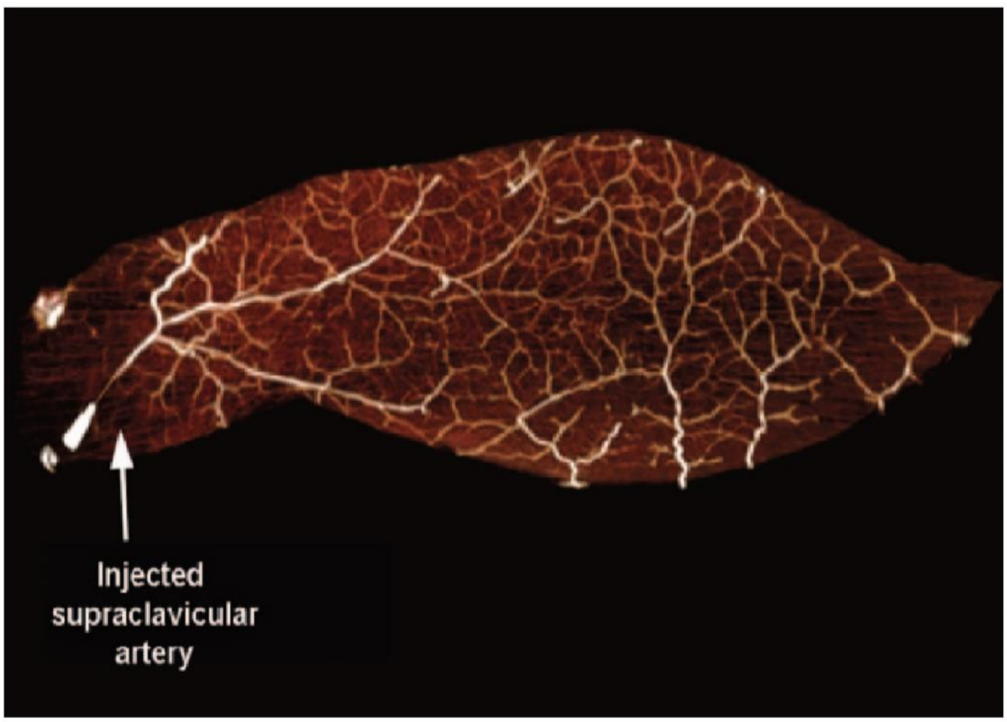

Figure 8: Three-dimensional computed tomographic angiogram of a supraclavicular flap (anteroposterior view). The flap was infused almost 100 percent (25).

1.5. Clinical applications of the supraclavicular flap

1.5.1. Dissection technique of the supraclavicular flap

The flap was raised from its lateral to its medial portion. Skin, subcutaneous tissue and fascia were elevated en block with the axillary running supraclavicular vessels, which may anastomose with cutaneous branches of the posterior circumflex humeral in its distal part. The surgical plane was carried down to the deep fascia, which was included into the dissection. Reaching the medial part of the flap, care has to be taken to correctly identify the accessory nerve, which has to be preserved, and the supraclavicular vessels, which most often arise from the superficial transverse cervical artery. these vessels emerge beneath or lateral to the posterior part of omohyoid muscle and can be identified easily by trans illuminating the flap in its medial aspect. A concomitant vein was seen in all cases. Finally, the medial portion of the flap was dissected ,and the complete fasciocutaneous flap was mobile on its vascular pedicle allowing 180-degree angle of rotation on the vascular axis .The flap can be raised in one stage without delay (26).

1.5.2. Supraclavicular flap application for head and neck reconstruction

In most of the researches the clinical use of this flap described as a pedicled flap for cervicofacial defect reconstruction, whether to a cutaneous defect or to an aero-digestive defect reconstruction in the head and neck as a substitute for a free flap, Figure 9.

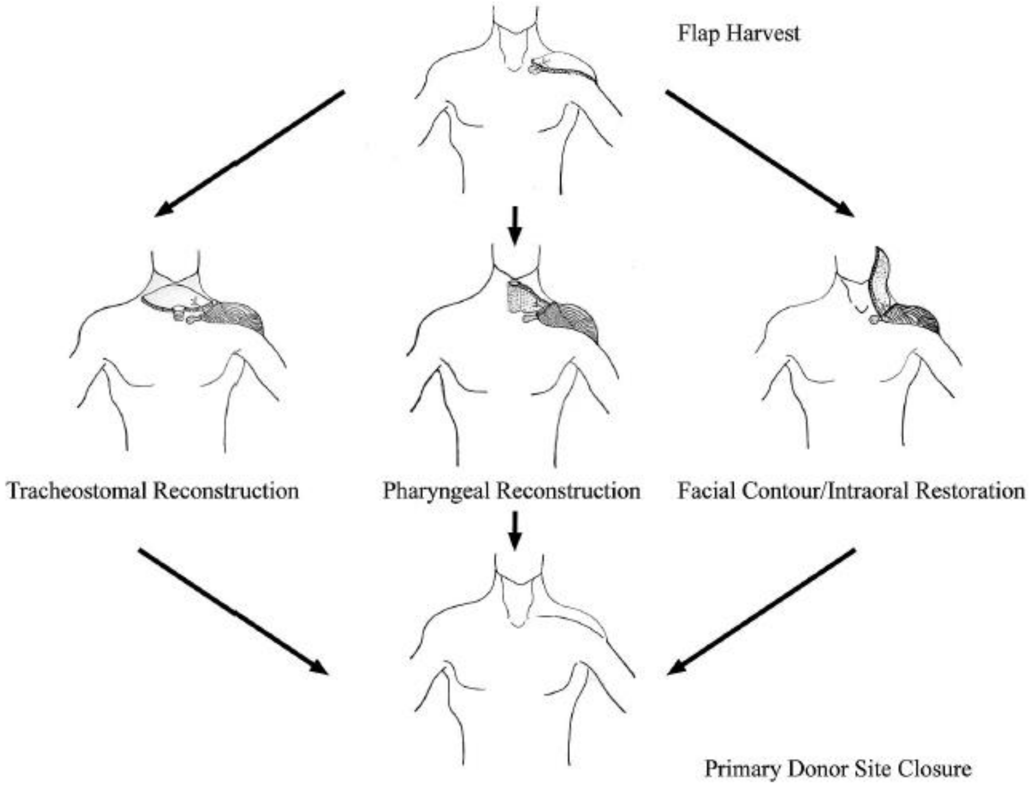

Figure 9: the clinical application of supraclavicular artery flap demonstrated (18).

1.5.3. Supraclavicular flap application for reconstruction of other parts of body

Mizerney et al and Cordova et al. ,introduced the theoretical usage of a small skin island in the supraclavicular area as a free flap (56, 58). However, Pallua et al transferred the supraclavicular artery flap as a free flap in two patients for reconstruction of traumatic soft-tissue defects in the hand and the foot (35).

Chapter

2

Hypothesis

and

Objectives

2. Hypothesis and Objectives

2.1. Hypothesis of the project

2.1.1. Part 1 of the project

To find the ideal technique for the preoperative mapping of the supraclavicular artery perforator flap.

2.1.2. Part 2 of the project

To assess the relationship between the characteristics of pedicled supraclavicular flap and distal end necrosis of the flap.

2.2. Objectives

2.2.1. Part 1 objectives

- To define the precise vascular boundary of the supraclavicular artery flap, through the information given by imaging techniques.

2.2.2. Part 2 objectives

- To determine the safe survival length of the supraclavicular artery flap.
- To increase the survival length of the supraclavicular artery flap through modification procedures.

Chapter

3

Patients and Methods

3. Patients and Methods

3.1. Part 1, Study of imaging findings of supraclavicular artery perforator flaps

3.1.1. Study design

An analytical study of imaging techniques used in preoperative mapping of supraclavicular artery perforator flap.

3.1.2. Venue of the study

This study was conducted in the Burns and Plastic Surgery Department in Sulaimaniah Teaching Hospitals in Sulaimani, Iraq and Plastic Surgery Departments of Hospital de la Santa Creu i Sant Pau and Hospital del Mar in Barcelona, Spain.

3.1.3. Inclusion criteria

All the patients with head and neck defect within the vicinity of the supraclavicular flap included. Furthermore patients from cardiac center, and other specialties that required an imaging tests in the supraclavicular region who have no burns and laceration injury to the area were included.

3.1.4. Imaging types, case numbers and data collection

In this study, the following six imaging modalities were used for supraclavicular vascular tree visualization:

1) Handheld Doppler (HHD)
2) Triplex ultrasound (TU)
3) Computed Tomography Angiogram (CTA)
4) Magnetic Resonance Angiography' (MRA)
5) Digital Subtraction Angiography (DSA)
6) Indocyanine Green Fluorescent Angiograms (ICGA).

A total of 74 cases were studied, they were aged between 19 and 85 years (mean age of 49.26 years, Standard Deviation 11.59), 32 males and 42 females, Table 1. Data collection involved both prospective and retrospective review of the imaging results performed for the included cases between July 2013 and February 2017. Informed consent was individually obtained from each prospective patients.

The results obtained were then subjected to statistical analysis to compare the feasibility of the all six imaging techniques in identifying the site of perforators of the supraclavicular artery, and mapping of the supraclavicular artery in relation to the surrounding anatomical structures. Statistical Package for the Social Science (SPSS) software was used for data analysis.

The site of the perforators marked as 'Yes' if the modality identified the site of any perforator on the skin of supraclavicular area, and marked as 'No' if the imaging technique failed to identify any perforator site.

Identification of the course of the supraclavicular artery measured as 'Complete', 'Partial' and 'No'.

'Complete' course is marked if the modality showed the complete course of the vessel from its origin to its subcutaneous course distal to the perforators. While 'Partial' course is regarded if the technique showed part of the course of the supraclavicular artery, and 'No' is marked if the imaging did not show any part of the vessel.

The Mapping of the supraclavicular artery is also measured as 'Complete', 'Partial,' and 'No'. 'Complete' mapping is marked if the modality showed the complete course of the *vessel in three dimensions in relation to the surrounding anatomical structures from its origin to its subcutaneous course distal to the perforators.

‘Partial’ mapping is selected if the imaging technique showed part of the course of the *supraclavicular artery in three dimensions in relation with the surrounding anatomical structures, or showed the subcutaneous course of the vessel starting from the perforators. And finally, ‘No’ mapping is marked if the imaging failed to show any part of the vessel.

Table 1:

This table shows the breakdown of this study's participants by number, age, and sex under the six different imaging techniques.

Modality	No of Patients	Age (Years)	Sex (Male, Female)
HHD	21	22– 85 (mean:48.3)	Male: 6 (28.57%) Female: 15 (71.43%)
TU	10	19 –44 (mean: 31.70)	Male: 3 (30.00%) Female: 7 (70%)
CTA	10	27-72 (mean: 42.00)	Male: 4 (40.00%) Female: 6 (60.00%)
MRA	10	26-82 (mean: 56.50)	Male: 6 (60.00%) Female: 4 (50.00%)
DSA	15	35-83 (mean: 65.06)	Male: 13 (13.33%) Female: 2 (86.67%)
ICG	8	42-65 (mean: 52.00)	Male: 0 (0.00%) Female: 8 (100%)

3.1.4.1. Handheld Doppler sonography (HHD)

In this group 21 Patients (25 sides) were included for assessment of the HHD technique, twelve were post-burn patients and nine were cancer patients, and Hand Held Doppler (Minidop ES-100VX, Hadeco, BT8M05 probe, and Biflow 4, Hadeco, BT8M05 probe) used.

In all the patients, supraclavicular flaps used for reconstruction of the tissue defects in the head or neck during the operations in the Burns and Plastic Surgery Department in Sulaimaniah Teaching Hospitals in Sulaimani, Iraq and Plastic Surgery Departments of Hospital de la Santa Creu i Sant Pau and Hospital del Mar in Barcelona, Spain.

HHD was the sole or one of the imaging techniques performed as a guide to flap design and dissection in each of these patients.

The data collected assessed the accuracy of the HHD findings preoperatively with the site of the main perforators of the flap pedicle found intraoperatively.

3.1.4.2. Triplex ultrasound (TU)

In this group 10 individuals (7 volunteers and 3 patients who considered for operation) been assessed to visualize supraclavicular vessel and its perforators on (17 sides) with Triplex ultrasound, vascular mapping was done with high sensitivity setting color Doppler then confirmation of arterial flow done with pulse Doppler in real time. MINDRAY DC8- L14-6NE and GE logic 6- 11L Ultrasound machines were used, at the radiology center, at the Sulaimaniyah teaching hospital in Sulaymani, Iraq.

The machine can identify the underlying vascular tree, and it also shows if the perforator has continuation with transverse cervical artery and deeper system.

3.1.4.3. Computerized Tomography Angiogram (CTA)

CTA of 10 patients (20 sides) studied at CT unit of the Cardiac center of Sulaimaniyah teaching hospital in Sulaimani, Iraq. Five of the patients had CTA of the neck region taken for different health problems with the arm in adducted position during the scan, 5 patients were burns and plastic surgery patients, in whom the burn involved the neck and part of the face and trunk, sparing the area of the scans and were considered candidates for surgery.

For this technique, Philips Brilliance 64 CT scanner used, and 60 to 70ml of Optiray containing 350mg/ml organically bound Iodine contrast was used for the whole procedure. The scanner enabled the generation of slices of thinner than 1 mm in all planes.

3.1.4.4. Magnetic Resonance Angiography (MRA)

We reviewed MRA of 10 patients (20 sides) who had this imaging technique performed for different medical indications in which the neck and supraclavicular region were shown.

They were performed in the imaging department of Hospital de la Santa Creu i Sant Pau in Barcelona, Spain. 3T MR machine was used. The contrast used was IV Dotarem 0.5mmol/ml at the dose of 0.2ml/kg injected into a superficial vein of the upper extremity at a rate of 2 ml/sec, followed-up by a 20 ml saline flush at the same rate; Image acquisition time was 15 to 20 seconds.

3.1.4.5. Digital Subtraction Angiography (DSA)

Fluoroscopy and subtraction angiography was performed on 15 patients (16 sides included). Thirteen of the patients were cardiac patients in whom the cardiologist performed PCI procedure and informed consent were taken to perform 2 or more

Fluoroscopy views in the shoulder region, during the removal of the catheter after the PCI procedure.

Two patients were burn patients in which the burn involved the neck and chest, but sparing the skin of shoulder region and therefore were considered candidates for surgery utilizing the supraclavicular artery flap.

Seimens and GE machines were used for this procedure, which required 5 - 6 seconds of radiation time and 15ml of diluted Optiray 350mg/ml organically bound Iodine contrast per each fluoroscopy view in the Cardiac center of Sulaimaniyah teaching hospital in Sulaimani, Iraq.

In 13 cardiac patients, the right radial artery used for access. After finishing the catheterization of the coronary artery, the catheter was withdrawn into the subclavian artery and the dye was then injected to show the branches of the thyrocervical trunk of the subclavian artery.

The left radial artery was used as an access in one burn patient but after spasm of the vessel, the right femoral artery used to gain access to the left subclavian artery where the flap was planned. On the other burn patient, the right femoral artery was used as an access point to both the right and left subclavian arteries to illustrate the course of the arteries with their branches.

3.1.4.6. Indocyanine Green Fluorescent Angiogram (ICGA)

Eight cases (15 sides) were considered for this imaging technique. Seven patients had breast reconstruction after mastectomy performed in whom ICG angiogram was used to assess flap vascularity. Consent was taken to view both shoulder regions at the time of breast flap scan in of Hospital de la Santa Creu i Sant Pau in Barcelona, Spain.

The other patient had a tumor of the face. This technique was used to sketch the vascular tree of the left supraclavicular artery to design the supraclavicular artery flap for reconstruction of the facial defect on one patient with skin cancer on the face, after wide excision of the lesion at of Hospital de la Santa Creu i Sant Pau in Barcelona, Spain.

ICG 25mg vials were reconstituted in 5ml Normal Saline, then 0.3mg/Kg were injected intravenously as a bolus, and the Photodynamic eye (PDE) near-infrared machine used as angiogram to visualize the superficial blood vessels, and the site of the perforators vascular branches marked on the skin with a marker pen in the Real Time of the Angiogram.

3.2. Part 2, clinical applications of supraclavicular artery perforator flaps

3.2.1. Study design

Clinical case series assessment of the relationship between characteristics of pedicled supraclavicular flap and distal end necrosis of the flap.

3.2.2. Venue of the study

This study was conducted in the Burns and Plastic Surgery Department in Sulaimaniah Teaching Hospitals in Sulaimani, Iraq and Plastic Surgery Departments of Hospital de la Santa Creu i Sant Pau and Hospital del Mar in Barcelona, Spain.

3.2.3. Inclusion criteria

All the patients that had undergone head and neck wound reconstruction with pedicled supraclavicular artery flap, in both centers in the time frame mentioned below were included in this study.

3.2.4. Case numbers, defect types and data collection

In the time frame of July 2013 and February 2017, 21 patients underwent reconstruction with supraclavicular flap for head and neck defects following the release and excision of burn contractures and wide excision of tumors. The procedures were performed in 15 female and 6 male patients, which had a mean age of 48.3 years.

A total of 25 flaps were used for 21 patients, in which 4 of these cases had bilateral flap reconstruction. Overall, 11 of the flaps were harvested from the right side of the neck whereas the remaining 14 flaps were taken from the left side. Of the 21 patients that underwent reconstruction, 12 of them had post-burn neck contractures and scarring, which were excised and the defects were then reconstructed using the supraclavicular flap. Whereas, the other 9 patients underwent supraclavicular flap reconstruction for the defects following wide excision of head tumors.

As smoking could be a factor, which might affect the vascularity of the flaps. In this study, it was noted that all the male patients were ex-smokers or they had quit smoking prior to the operations. Whereas, all the female patients were non-smokers.

All the surgical procedures including flap harvesting and the reconstruction were performed under General Anesthesia. Different imaging techniques such as Hand Held Doppler, Computerized Tomography Angiogram, Fluoroscopy angiogram and Indocyanine green angiogram were used preoperatively or intraoperatively for some of the patients as mentioned in Table 2. In addition, modification techniques such as delay procedures and tissue expansion were also performed as a separate procedure in some of the flaps Table 2.

Table 2:

Shows patient's age, sex, side, the dimension of the flaps (length and width), defect type and site, distal flap end necrosis, imaging tests, pre-expansion or/and delay procedures.

Patient	Age (Years)	Sex (Male, Female)	Side (Right, Left)	Dimensions of the flap	Defect type and site	Distal end necrosis (yes in cm or no)	Imaging tests or preliminary procedures (delay or tissue expanders)
1	53	Male	Left	7 x 14	Burn contracture in neck	No	HHD
2	22	Male	Right Left	7 x15 7x 15	Burn contracture in neck	No No	HHD HHD
3	35	Female	Right Left	8 x 23 10 x 25	Burn contracture in neck	No Yes ,2.5cm	HHD HHD, DSA, and Tissue expander
4	27	Female	Right	8 x 25	Burn contracture in neck	No	HHD, and TU
5	50	Female	Left	11 x30	Wide excision of recurrent SCC in Left temple	No	HHD, TU, and Delay

6	40	Female	Right	6 x 12	Burn contracture in neck	No	HHD, and TU
7	37	Female	Left	5 x 12	Burn contracture in neck	No	HHD
8	26	Female	Right	10x 35	Burn contracture in neck	Yes , 6cm	HHD, and Delay procedure
9	30	Female	Left	9 x 25	Burn contracture in neck	No	HHD, CTA ,Tissue expander + delay
10	55	Male	Left	8 x 17	Burn contracture in neck	No	HHD, and CTA
11	27	Female	Left	8 x 18	Burn contracture in neck	No	HHD , and CTA
12	35	Female	Right Left	7 x 15 7x 17	Burn contracture in neck	No No	HHD HHD
13	23	Female	Right Left	10 x 25 11 x 27	Burn contracture in neck	No No	HHD, Tissue expander HHD, Tissue expander
14	76	Female	Left	8.5 x 27	basal cell carcinoma in check	No	HHD, and ICG preop

15	50	Female	Right	6x17	mastoides exposition complication of) (Neurosurgery	No	HHD, and CTA
16	85	Female	Right	9x21	SCC intraparotid metastasis	No	HHD ICG evaluation of flap, normal
17	70	Female	Left	8x23	malignant tumor of parotid gland	2 cm necrosis	HHD ICG evaluation, normal
18	76	Female	Left	7x16	SCC in check	No	ICG evaluation normal
19	78	Male	Right	10x27	SCC intraparotid metastasis	No	HHD
20	71	Male	Right	7x20	Dermatofibrosarcoma protuberans in neck	No	HHD, ICG evaluation normal
21	49	Male	Left	7x18	Sarcoma metastasis in neck	No	HHD

Chapter

4

Results

4. Results

4.1. Results of part 1 of the study

4.1.1. Handheld Doppler (HHD)

The results of HHD imaging shown in Table 3. The site of the main perforators in 20 (80%) flaps were identified correctly and found to be compatible with the intraoperative site of the perforators, Figure 10 a, Figure 10 b, Figure 10 c, Figure 11 a, Figure 11 b, and Figure 11 c.

Table 3

Result of six different imaging techniques used for identification of the site of the main perforators, course, and anattomical mapping of supraclavicular artery.

Modality	No. of Sides (Right and Left)	Identification of the site of the perforator (Yes, No)	Identification of the course of supraclavicular artery (Complete, Partial, No)	Mapping of the supraclavicular artery (Complete, Partial, No)
HHD	25 (Right 11, Left: 14)	Yes: 20 (80%) No: 5 (20%)	Complete: 0 (0%) Partial: 0 (0%) No: 25 (100%)	Complete: 0 (0%) Partial: 0 (0%) No: 25 (100%)
TU	17 (Right 14, Left: 3)	Yes: 9 (52.94%) No: 8 (47.06%)	Complete: 0 (0%) Partial: 11 (64.70%) No: 6 (35.30%)	Complete: 0 (0%) Partial: 0 (0%) No: 17 (100%)
CTA	20 (Right 10, Left:10)	Yes: 12(60%) No: 8 (40%)	Complete: 9 (45%) Partial: 6 (30%) No: 5 (25%)	Complete: 9 (45%) Partial: 6 (30%) No: 5 (25%)

MRA	20 (Right 10, Left:10)	Yes: 0 (0%) No: 20 (100%)	Complete: 0 (0%) Partial: 0 (0%) No20 (100%)	Complete: 0(0%) Partial: 0 (0%) No: 20 (100%)
DSA	16 (Right 14, Left:2)	Yes: 0 (0%) No: 16 (100%)	Complete: 0 (0%) Partial: 10 (62.50%) No6 (37.50%)	Complete: 0 (0%) Partial: 0 (0%) No: 16 (100%)
ICG	15 (Right 8, Left:7)	Yes: 9 (60%) No: 6 (40%)	Complete: 0 (0%) Partial: 9 (60%) No: 6 (40%)	Complete: 0 (0%) Partial: 9 (60%) No: 6 (40%)

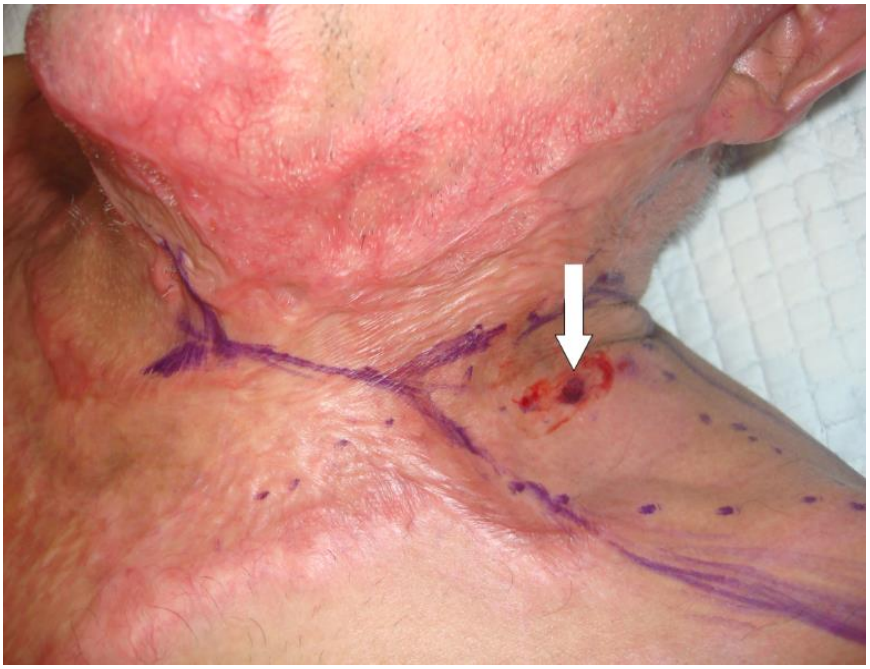

Figure 10 a: Post burn contracture and hypertrophic scar of the neck. The site of the perforator identified with HHD and marked (the arrow).

Figure 10 b: The left supraclavicular flap raised on the supraclavicular artery perforator which was Identified by HHD preoperatively (tip of the scissors pointed to).

Figure 10 c: Flap inset done, and the flap survived on the HHD identified perforator

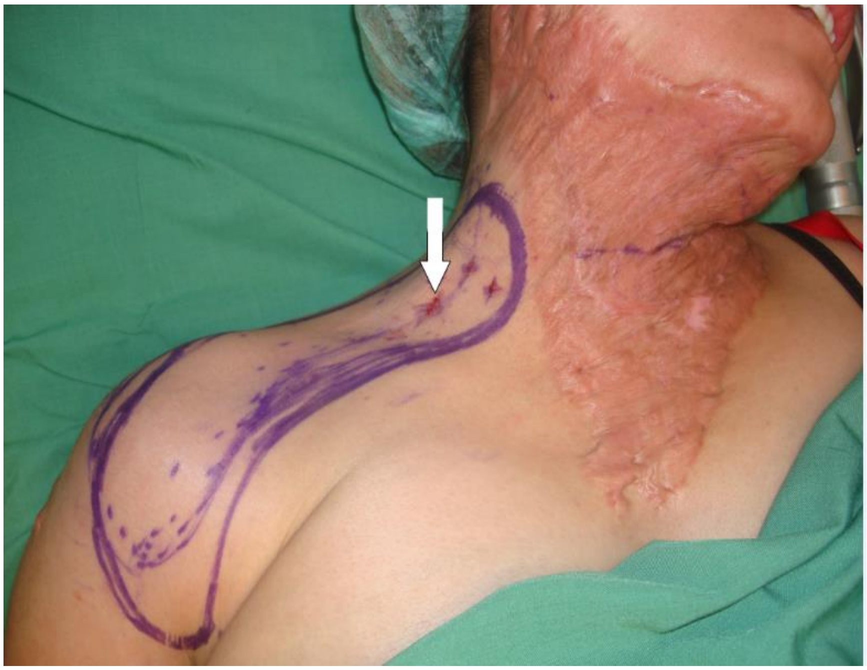

Figure 11 a: Post burn contracture and hypertrophic scar of the neck. Right supraclavicular flap designed and site of the main perforator identified by HHD and marked (the arrow).

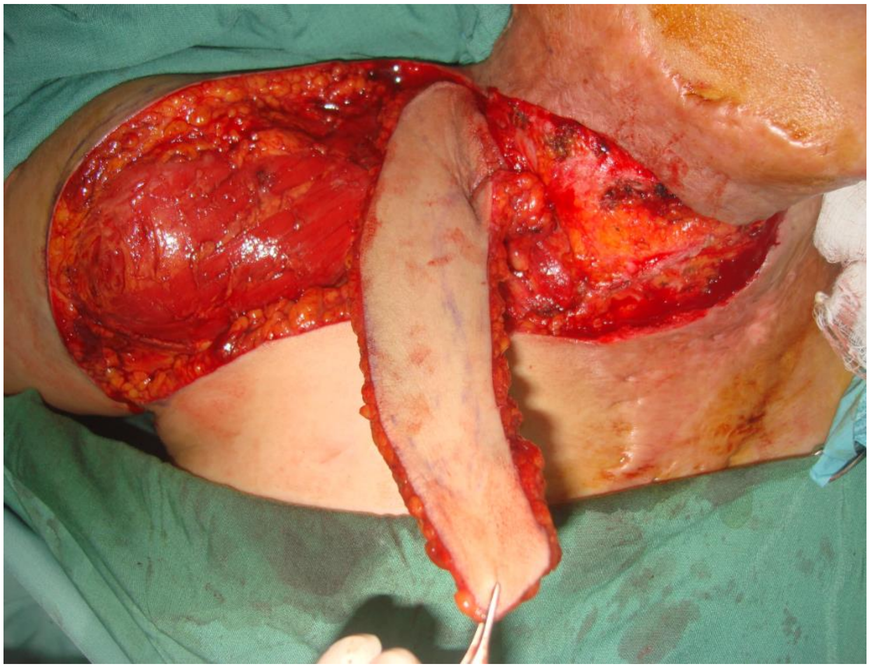

Figure 11 b: The contracture released and the supraclavicular flap raised on the preoperatively identified main perforator.

Figure 11 c: Flap inset done and the whole flap survived on the HHD identified perforator.

4.1.2. Triplex Ultrasonography (TU)

The results of using Triplex Scan are shown in Table 3. Transverse cervical artery and supraclavicular branch clearly visualized Figure 12 a, Figure 12 b. A vascular branch as small as 0.5mm could be viewed with this technique Figure 12 c.

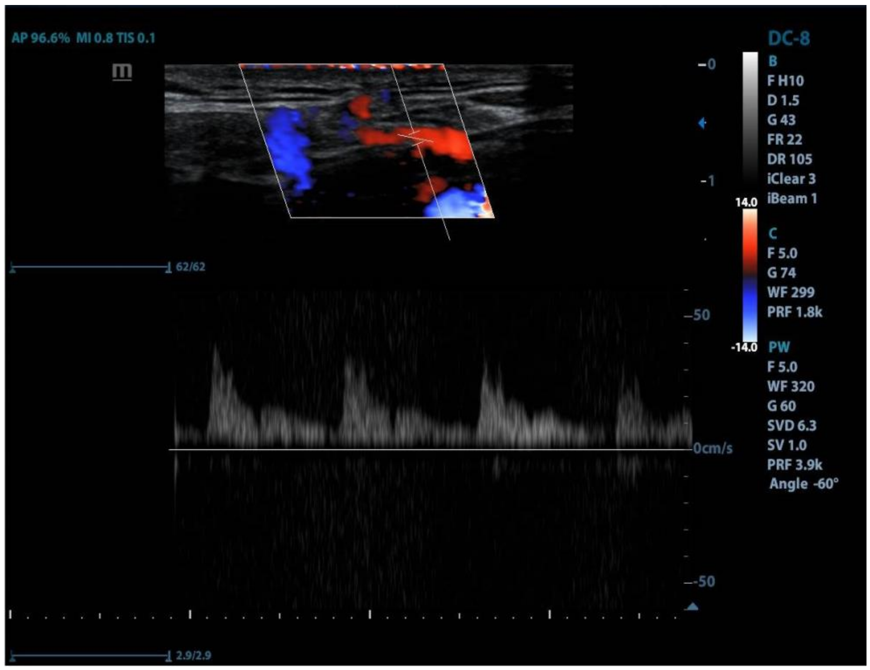

Figure 12 a: The transverse cervical artery and supraclavicular artery shown in red color by Triplex Ultrasonography and spectrum of the pulsation shown below.

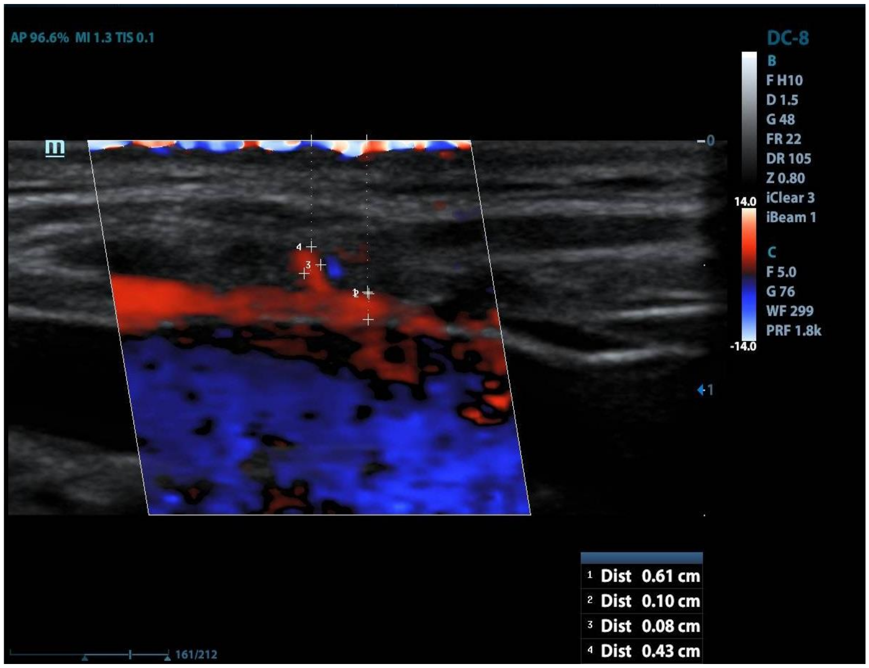

Figure 12 b: Triplex Ultrasonography shows the transverse cervical artery and supraclavicular branch. The size of supraclavicular artery is 0.8 mm and 0.43cm distance from the skin surface.

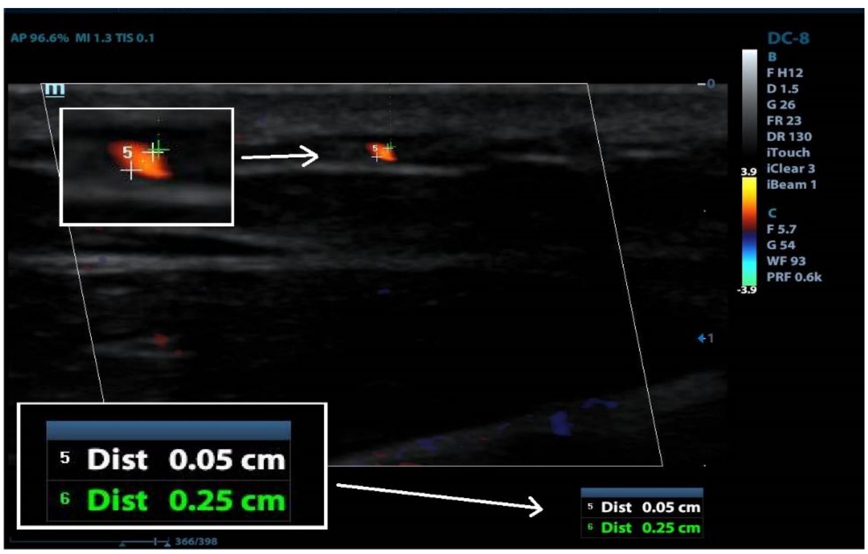

Figure 12 c: Triplex Ultrasonography showed the supraclavicular artery as small as 0.5 mm (zoom in).

4.1.3. Computerized Tomography Angiogram (CTA)

The results of using CTA are shown in table 3. Supraclavicular artery perforator to skin marked and mapped at a given point in 3 dimensions. Figure 13 a, and Figure 13 b.

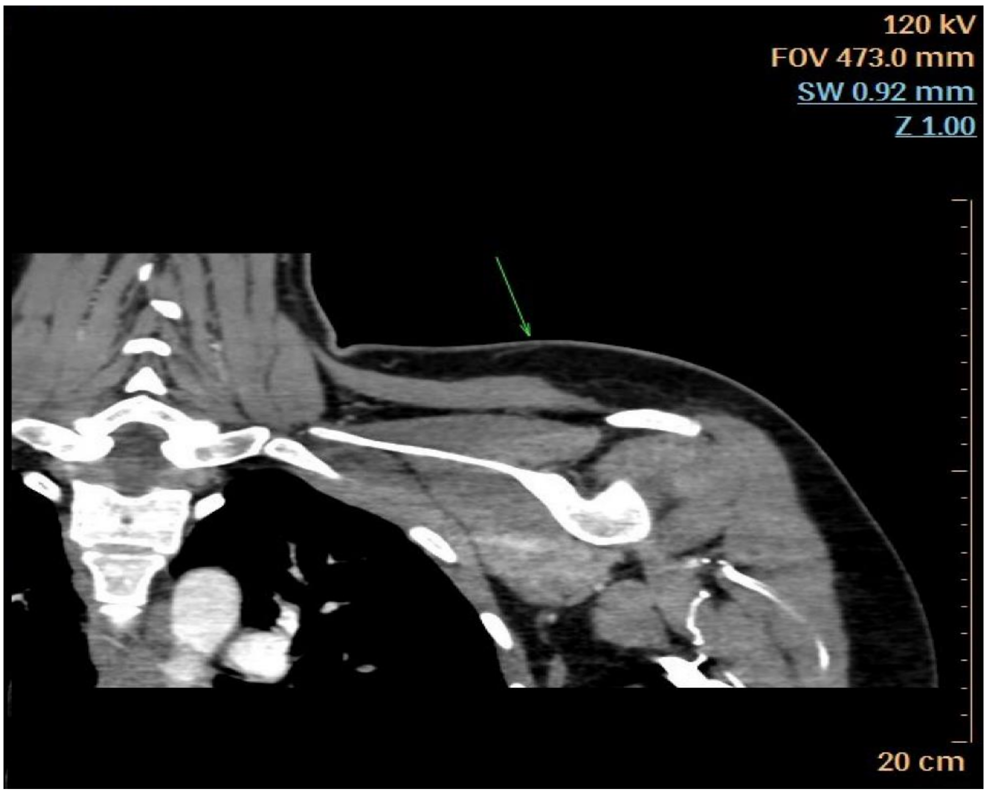

Figure 13 a: Computerized Tomography Angiogram (CTA) showed the site of supraclavicular artery perforator to the skin (the arrow).

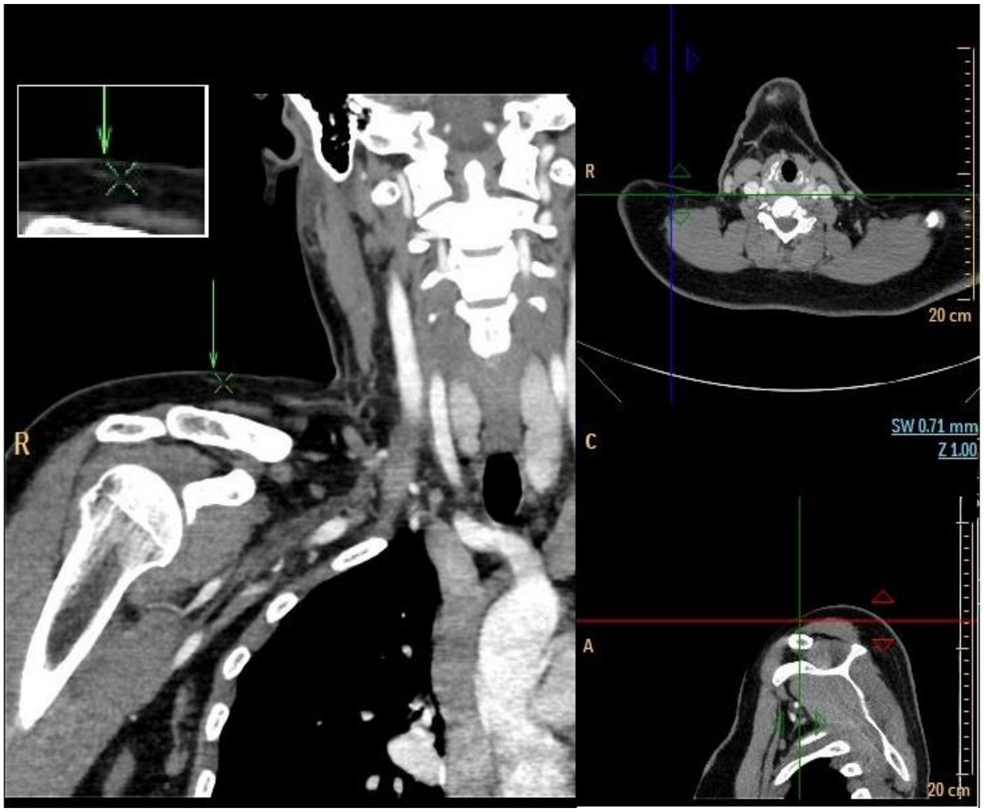

Figure 13 b: Computerized Tomography Angiogram (CTA) showed the vascular tree starting from thyrocervical trunk, transverse cervical artery, and supraclavicular artery perforator. A point on the supraclavicular artery marked on coronal section and shown by a cross cursor on the cross section and sagittal section.

4.1.4. Magnetic Resonance Angiography (MRA)

The result of the review of the MRA shown in Table 3. The course of the transverse cervical artery shown in Figure 14 while course of the supraclavicular artery is not visible.

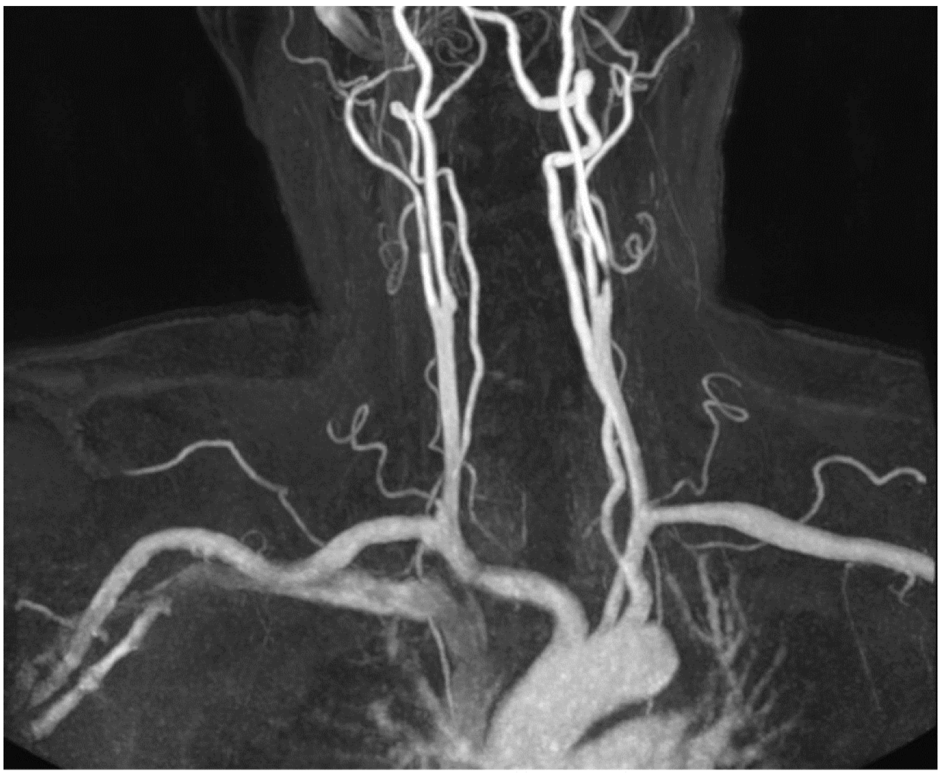

Figure 14: Magnetic Resonance Angiography (MRA): The supraclavicular artery course and perforator site couldn't be visualized clearly.

4.1.5. Digital Subtraction Angiography (DSA)

The results of using DSA are shown in Table 3. Figure 15 shows the vascular tree image in DSA mode.

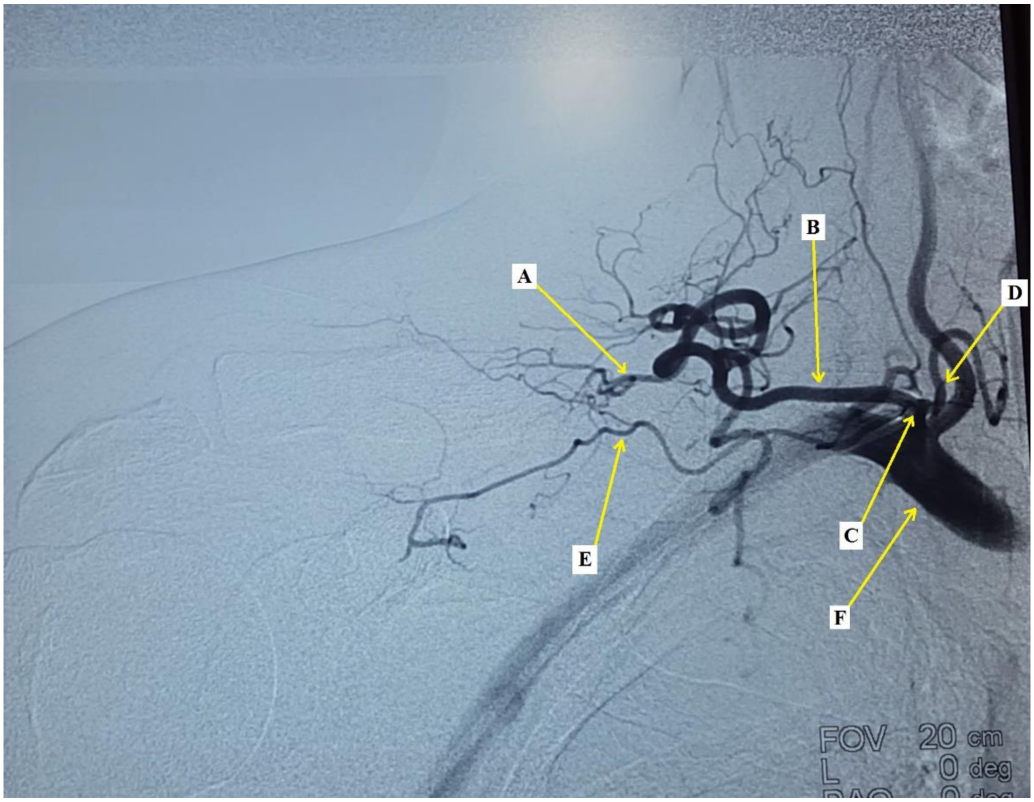

Figure 15: Digital subtraction angiogram DSA shows vascular tree of supraclavicular artery from its origin in subtraction mode. A: Supraclavicular artery, B: transverse cervical artery, C: thyrocervical trunk, D: suprascapular artery, E: inferior thyroid artery, F: subclavian artery.

4.1.6. Indocyanine Green Fluorescent Angiograms (ICGA)

The results of using ICGA are shown in Table 3. Intraoperative ICGA image of supraclavicular artery perforator flap design on the ICG identified vessels, dissection and inset shown in Figure 16 a, Figure 16 b, Figure 16 c, and Figure 16 d.

Figure 16 a: Indocyanine Green Fluorescent Angiogram (ICGA) shows the site of perforator and course of the supraclavicular artery distal to the perforator (the arrow).

Figure 16 b: the left supraclavicular flap been dissected and raised on the ICG identified supraclavicular artery perforator.

Figure 16 c: trans illumination shows the ICG identified supraclavicular vessel inside the supraclavicular flap.

Figure 16 d: left supraclavicular flap used for reconstruction of a defect on the face after wide excision of a tumor. The flap completely survived on the ICG identified vessels.

The statistical analysis of the results were worked out by Cross tabulation and Likelihood Ratio Chi-Square for all three paremeters (identification the site of the perforators in the supraclavicular region, course of supraclavicular artery, and mapping of supraclavicular artery in relation to surrounding anatomical structures) for all six imaging techniques, and showed statistically significant ratio (P value < 0,001).

4.2. Results of part 2 of the study

The result of the study shown in (Table 2). The size of the flaps varied in length and width according to the patient's need. On average the length ranged from 12-35 cm with a mean length of 20.76 cm (Std. deviation 6.01), whereas the width of flaps ranged from 5 -11 cm, resulting in a mean width of 8.06 cm (Std. deviation 1.59).

Overall 25 flaps were raised in 21 patients, and there was no total flap loss, however, 3 of the flaps (12%) resulted in distal end necrosis. The lengths of these necrotic flaps were 23, 25 and 35 cm with distal necrosis of 2, 2.5 and 6cm respectively (Table 2).

The donor sites of 20 flaps closed directly, while donor sites of case 1, 5, 9. 14, and 19, from Table 1, required split-thickness skin grafting in the area which was not possible to be closed directly.

The 3 flaps with distal end necrosis were managed accordingly. Two flaps with a smaller defect were managed with dressings and secondary healing without sequelae, while the flap with bigger necrosis required debridement, and approximations.

4.2.1. Case presentations

Case 1 :

(case 15 from Table 2): 50 years old female had mastoid exposition with osteomyelitis as a complication of neurosurgery team (pontocerebellar angle meningioma approach). Figure 17 a and Figure 17 b. The defect has been reconstructed with a right supraclavicular flap size 17 X 6 cm., Figure 17 c, and Figure 17 d.

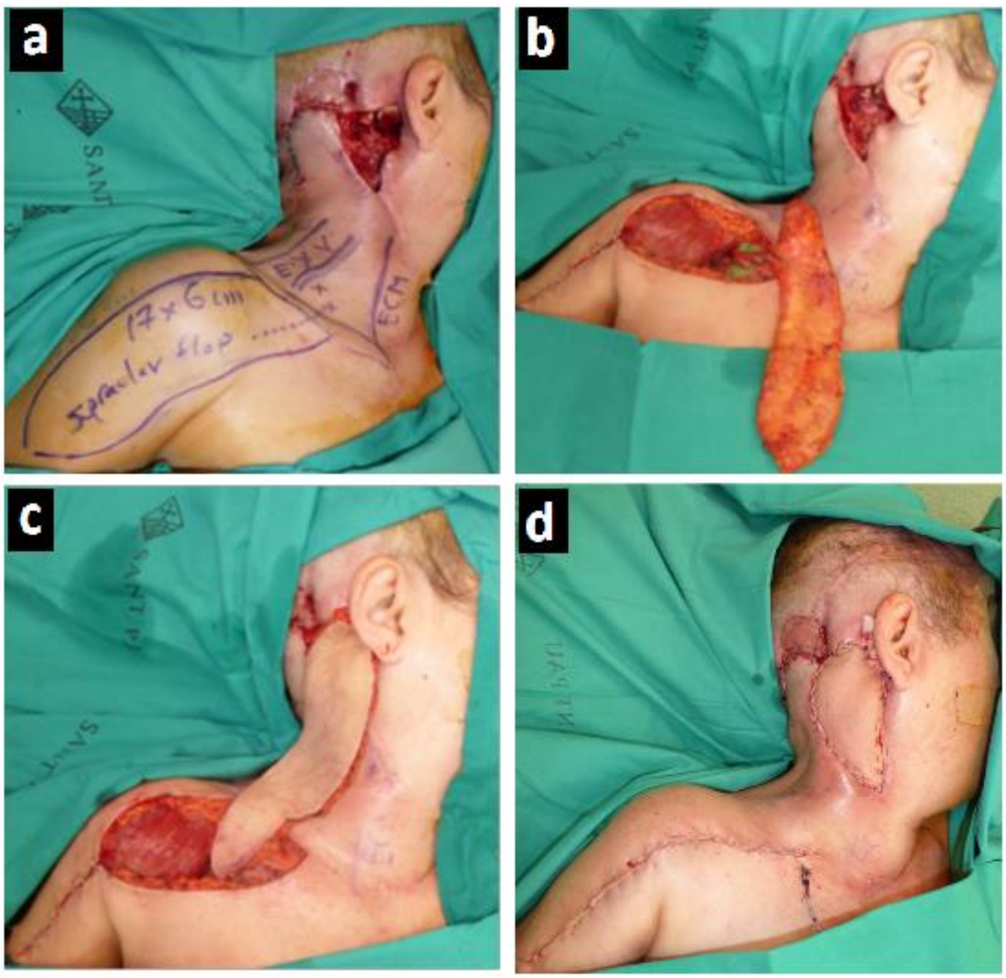

Figure 17: Figure 17 a: intraoperative view of the defect that progressed rapidly and the right supraclavicular flap designed, Figure 17 b: the flap raised, and the supraclavicular vessel isolated on the green background, Figure 17 c: the flap rotated in to the defect, Figure 17 d: the flap inset done and the donor site closed directly.

Case 2:

(case 3 from Table 2): 35 years old female, post-burn hypertrophic scar and contracture on the neck and chest, Figure 18 a. Three surgical procedures in different time were performed. The first surgical procedure was a partial excision of the neck scar and 8 x 23 cm right supraclavicular flap used to fill the defect. The second procedure included left pre-expanded supraclavicular flap and also tissue expander colocation under the right supraclavicular flap in the neck, Figure 18 b . The third procedure included the excision of the remaining scar, expanders removed, 10 x 25 left supraclavicular flap raised, both flap inset done, and donor sites were closed directly Figure 18 c , and Figure 18 d. Further scar revision and Z plasty in the neck performed as a separate minor procedure.

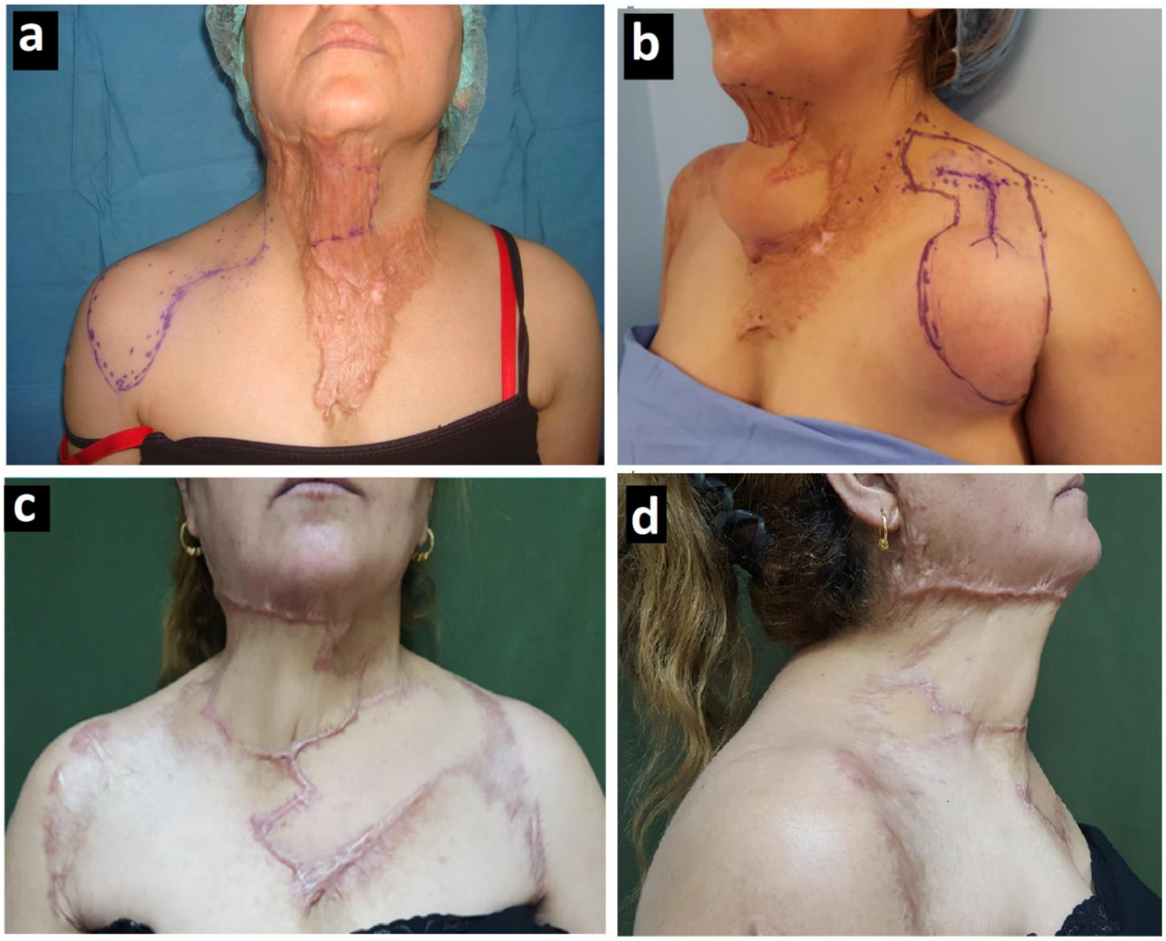

Figure 18: Figure 18 a: post-burn hypertrophic scar and contracture on the neck and chest. Figure 18 b: left pre-expanded supraclavicular flap and also tissue expander colocation under the right supraclavicular flap in the neck. Figure 18 c, and Figure 18 d: post-operative view of the neck reconstruction with right and left supraclavicular flaps and donor sited closed primarily.

Case 3 :

(case 5 from Table 2): 50 years old female, with a fourth recurrence of squamous cell carcinoma (SCC) of the scalp and temple, involved left temporoparietal area and left auricle Figure 19 a. the CT scan showed infiltration of the outer table of the skull. In the first surgical session, a flap of 11 cm x 30 cm was delayed to increase the survival length of the flap through the delay phenomena. In a second stage (3 weeks later), multidisciplinary team of neurosurgeons, otolaryngologists, and plastic surgeons performed wide tumor excision including the auricle and part of the skull bone, and the defect was reconstructed with a supraclavicular flap of 11cm x 30 cm, and the donor site was covered with a split-thickness skin graft Figure 19 b, Figure 19 c, Figure 19 d, and Figure 19 e.

Figure 19: Figure 19 a : Squamous Cell Carcinoma (SCC) of the scalp and temple, involved left temporoparietal area and left auricle. Figure 19 b: the supraclavicular flap of 30 X 11 cm marked to be delayed. Figure 19 c: the flap of 30 cm length from the pedicle has been raised. Figure 19 d: the flap inset. Figure 19 e: 3 months' postoperative view.

Case 4:

(case 9 from Table 2): 30 years old female with post burn neck contracture Figure 20 a. A pre-expanded and delayed left supraclavicular flap 9 x 25 cm used for reconstruction after the neck scar excision Figure 20 b, Figure 20 c, and Figure 20 d.

Figure 20: Figure 20 a: post burn neck contracture. Figure 20 b. A pre-expanded and delayed left supraclavicular flap 9 x 25 cm has been raised for neck defect reconstruction after the neck scar excision. Figure 20 c, and Figure 20 d : 6 months postoperative view.

Case 5:

(case 14 from Table 2) 76 years old female with Cluster A disease and basal cell carcinoma in the left cheek Figure 21 a. The tumor was widely excised and the defect reconstructed with 27 x 8.5 cm supraclavicular flap. Intraoperative ICG evaluation was performed to mark the pedicle and design the flap. The donor site was closed with a split-thickness skin graft Figure 21 b, Figure 21 c, Figure 21 d, and Figure 21 e.

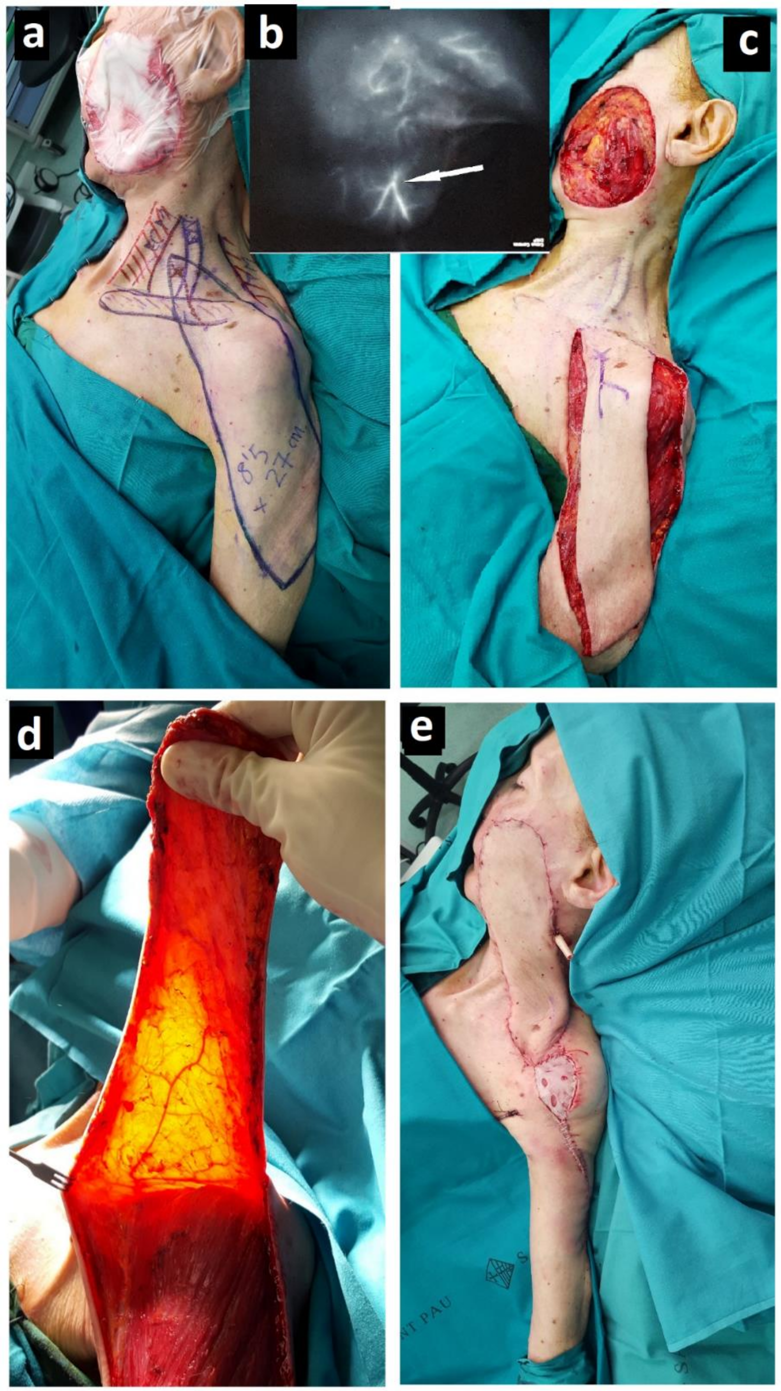

Figure 21: Figure 21a: basal cell carcinoma in the left cheek was widely excised, and a supraclavicular flap of 27 x 8.5 cm designed. Figure 21 b: Intraoperative ICG was performed to identify the pedicle. Figure 21 c: the vascular pedicle marked, the flap design adjusted accordingly and the flap raised. Figure 21 d: the transillumination of the flap shows the pedicle in the marked area. Figure 21e: the flap inset done and the donor site was closed with a split-thickness skin graft.

Cases of the flap necrosis:

(Case 3, 17, and 8 from Table 2): Three flaps from the total of 25 flaps , had distal end necrosis, Figure 22 a, Figure 22 b, and Figure 22 c. Flap a and b were managed with dressings and secondary healing without sequelae, while flap c required debridement and approximations.

Figure 22: Figure 22 a, Figure 22 b, and Figure 22 c : the 3 cases with distal end necrosis.

Chapter

5

Discussion

5. Discussion

5.1. Discussion Part one of the study

The supraclavicular island flap has the best color and texture match to the neck been widely used in head and neck reconstruction, but its vascularity remains unclear (16, 37) .

From the imaging techniques used for mapping the supraclavicular artery in this study from simple noninvasive HHD to more invasive digital subtraction angiogram, the supraclavicular artery branch and perforators are mapped in different degrees of detail.

The handheld Doppler is useful for localizing the cutaneous perforators of the supraclavicular artery, but it's not suitable for vascular mapping. In this study, the predictive value for HHD was 80 % in identifying the site of main perforators compared with the findings intraoperatively. This may be due to the thin subcutaneous tissue of the supraclavicular region. Khan et al, in 2007 reported, a positive predictive value of only 52.4% for HHD in a series of 32 DIEP and 8 SGAP flaps, where the site of emergence of the perforators from the fascia is different from their location more superficially (62) . One of the limitations of HHD is that its sensitivity is restricted to superficial vessels. Yu et al in 2006 reported the limited sensitivity of HHD for deeper blood vessels (63). Also, Smit et al in a study in 2010 mentioned the shortcomings of HHD as it can’t specifically identify the vessel which produces the sound, and it tended to pick up signals from very small surrounding vessels other than the perforator (7, 64).

Although with Triplex sonography we could identify the transverse cervical artery, the supraclavicular branch and its perforators to the size of 0.5 mm in some cases, but the technique is highly operator dependent, which was also emphasized by Smit et al in 2010 (7). Masia et al in 2006, Smit et al in 2009 and Ogawa et al.

mentioned the disadvantages of Color Doppler as it does not reproduce a 3D image of the complete vascular anatomy in comparison with CT and MRI, so it's value in precise vascular mapping is limited (11, 13, 65, 66).

According to the results achieved in this study, the CT angiogram is at the top of the list of the imaging techniques to achieve the goal in preoperatively defining the course of the supraclavicular artery from its origin to its smaller branches fading away under the skin. Mathes et al in 2010, and Alonso et al in 2010 reported that CTA has been shown to be accurate in demonstrating the location, size, and course of musculocutaneous perforators as small as 0.3 mm and is less dependent on body habitus (67, 68). It has been used to identify the pedicle and design flaps in different parts of the body (7, 11, 13, 65, 68-74).

The limitations are inability to define the perforator perfusion zones, the radiation exposure and the vasospastic properties of the iodinated dye**,** which can make the accurate assessment of small caliber vessels difficult, as reported by Masia et al, Ogawa et al, and Rozen et al (11, 65, 75) .

With MRA the transverse cervical artery and the larger branches could be seen clearly in supraclavicular region, while the distal course of the supraclavicular artery and perforators were difficult to be reliably identified and accurately mapped. MRA was not as sensitive as CTA for depiction and mapping of smaller vessels reported by Alonso et al, Mathes et al, Chernyak et al, and Rozen et al (65, 68, 76, 77) . However, the value of MRA as mentioned by Smit et al, Fukaya et al, Kelly et al and Lohan et al is that could be used as a guide for flap design and dissection in a patient with a contraindication to radiation exposure (7, 12, 78, 79).

Digital subtraction angiography can show the vascular tree of the vessel completely from its origin to the very small branches, Video 1. It shows the course, the axiality, the size and state of filling of the vessel, also emphasized by Seres et al 2001 (80). However, it’s a 2 D technique. Even with several different views, one cannot actually map the vascular tree precisely according to its relation with other surrounding anatomical structures, Video 1. This type of imaging is the most invasive and demanding technique which uses the highest dose of radiation than all other techniques as also reported by Tan 2007 (81), and has all the risks of catheterization and iodinated contrast medium.

In this group ICG fluorescent angiography nicely demonstrated the supraclavicular artery perforators and subcutaneous course of the vessel distally to the perforators, Video 2. Indocyanine green allows one to quantify tissue perforator perfusion zones, and precisely mark the boundaries in a dynamic and real-time application of the imaging technique Video 2, with no risk of radiation, also described by Namikawa et al 2015 and Herz et al 2016 (82, 83). It can be used to map the superficial course of the vessel preoperatively and intraoperatively and is a helpful guide in flap design and decision making in the surgery, but the sensitivity is limited to the vessels in the superficial subcutaneous plane.

The strength of this study is that it compares the multiple commonly used imaging modalities, both invasive and noninvasive, with and without the necessity of radiation exposure.

The limitations of the present study are the small number of the patients included, due to the invasiveness and risk of radiation of some of the imaging techniques.

We recommend further investigation of the use of ICG angiography with a larger number of cases and to better determine the reliability and safety of this radiation-free imaging technique. Because this technique is limited to vessels that are superficially located, it is best suited for mapping the course of vessels in thin flaps as in the case of the supraclavicular flap due to the scant amount of overlying tissue in this area.

When the cost is taken into account, the imaging techniques cost differently.

Some of the techniques cost virtually nothing such as HHD, while some of the imaging modalities require sophisticated expensive machines and equipment which cost higher. It’s also worth mentioning that ICG angiogram costs less than CTA. when they were used to map the flap vessels.

Video 1.mp4

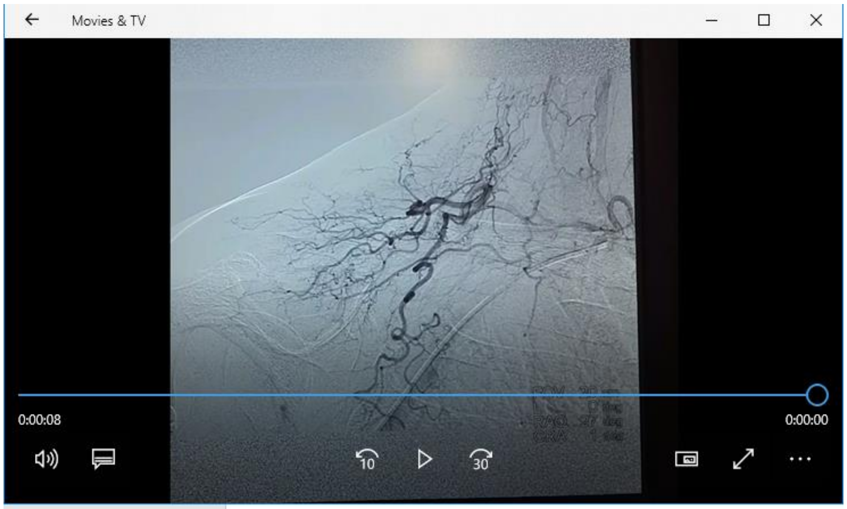

Video 1: Digital Subtraction Angiography. The iodinated contrast has been injected into the right thyrocervical trunk by an arterial catheter which was passed through the right radial artery to the right subclavian artery. The contrast is seen flowing to the branches of thyrocervical trunk, including the transverse cervical artery and supraclavicular artery. The vascular tree and the course of the vessels are clearly visualized, but as it is a two dimensional imaging modality, one cannot precisely map the course of the arteries in relation to the surrounding anatomical structures, limiting its usefulness.

Video 2.mp4

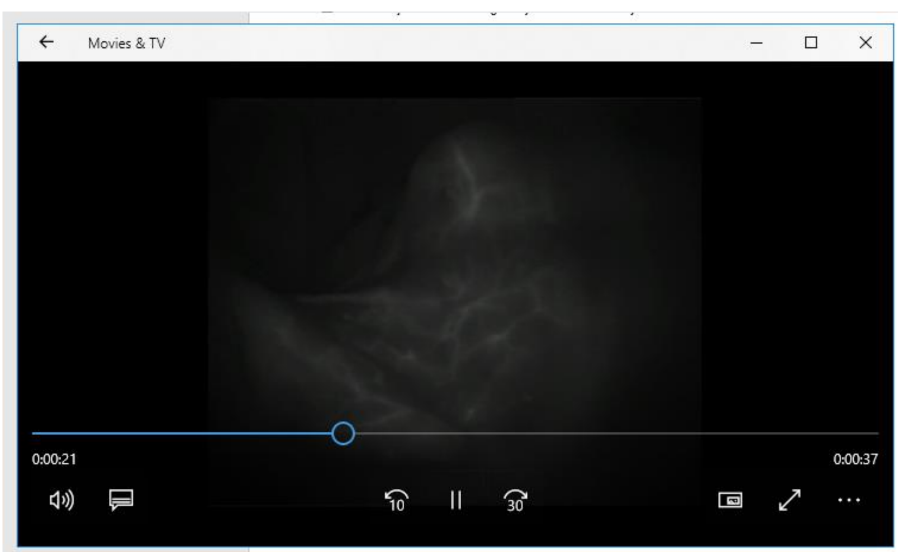

Video No.2: Indocyanine Green fluorescent angiography. After injection of the ICG intravenously, the dye passes through the systemic circulation. With the help of a photodynamic eye infrared camera, the ICG dye can be detected as it flows through the perforators and spreads throughout the superficial subcutaneous vessels. Here in this video, the vessels could be seen clearly in white on the screen when the dye flows through them. With this imaging modality, the subcutaneous vessels can be easily mapped.

5.2. Discussion Part two of the study

The results of this study have been analyzed to see the relationship between the flap length and distal end necrosis. According to the data obtained in the results section of this report, as the length of flap increases, the rate of distal end necrosis also increases. This was found to be true for flaps that exceeded 23 cm in length.

In this study 3 flaps (12% of the total) had distal necrosis, their length was (23cm, 25cm and 35 cm) with distal necrosis of 2cm, 2.5cm and 6cm respectively. This study has shown that there was no flap necrosis (0 %) for flaps that had a length below 23 cm, which comprises of 14 flaps (56 % of the total), whereas of the 11 flaps (44 % of the total) with size 23cm and above, 3 flaps resulted in distal flap necrosis, which makes (27.27%) of the 11 flaps.

The statistical analysis shows that the relation between flap length and distal necrosis has a significant P value of 0.039., which means that the length of the flap affects the distal vascularity.

From the literature review of supraclavicular flaps for head and neck reconstruction in PubMed search engine, 26 articles (4, 17-19, 26-30, 33, 37, 38, 40, 42-54, 60) were found that had used supraclavicular flaps for head and neck reconstruction and had clearly stated the length of flaps and their rate of necrosis (Table 4). The rate of necrosis is variable according to the size of the flaps, and only a few of the published articles clearly associated the rate of necrosis with the certain length of the flaps.

But the following articles have clearly discussed the relationship between the length of the supraclavicular flap and distal necrosis.

Ismail et al, in a study which involved 20 supraclavicular flaps ranged from 16 cm to 25 cm length (mean 21.7 cm), reported that 7 flaps (35%) showed partial distal necrosis, either in the form of superficial epidermolysis in 5 cases or full thickness necrosis of the distal two centimeters in 2 cases. They also reported that all their cases with distal necrosis, the flaps were 23 cm or more (40).

Ismail et al also recommend that supraclavicular flaps longer than 22 cm are not harvested immediately, and they recommend modification procedures such as flap expansion before harvesting (40).

Similarly, Kokot et al also in a study that involved 45 flaps, (mean length 21.4) reported flap length greater than 22 cm significantly correlated with flap necrosis, with a (P = .02) (46).

In a different article, Vinh et al reported, a unilateral supraclavicular flap with an average size of 22 x 10 cm can be elevated safety (37).

Also, Loghmani et al in a study with 41 flaps, The range of flap size was 18 ± 6 cm in length with 3 cases of distal necrosis, had also found that the supraclavicular flap can be safely elevated provided that it is within 20 x10 cm (48).

Similarly, Telang et al in their study found that the supraclavicular flap can be safely elevated within dimensions of 20cm × 10cm, and the use of tissue expansion greatly amplifies the total area available (50).

The results in the above discussed 5 articles, strongly back our results that the flap of 23 and above correlates with distal necrosis.

Although the results of a published article by Kokot et al contradicts the findings of the above-mentioned papers, that they had used 22 supraclavicular artery flaps ranging 16-28 cm length (mean length range of 21.8 cm), with partial skin flap necrosis occurred in 2 patients. In this article, it was published no statistical correlation found between flap necrosis and flap length, with a (P = 0.3), (47)

In this study the effect of the modification procedures (the delay and the tissue expansion) clinically not clear on the survival of the distal end of the flaps and statistically cannot be related due to the small sample size, but apparently the expansion procedures helped in closing the flap donor sites directly up to 11 cm width.

Table 4

Table 4 shows the articles, number of the flaps, length of the flaps in centimeters, and number of distal flap necrosis

Articles	No of flaps	Length of flap (range or mean) in cm	No. of flap with distal necrosis
Ismail et al 2016 (40)	20	25-16	2
Margulis et al 2017 (38)	16	20-35	1
Chen et al 2016 (42)	12	12-20	Non
Zhang et al 2015 (54)	10	8-12	2
Yang et al 2015 (51)	16	12-22	Non
Emerick et al 2014 (44)	16	6 to 15 (10.3 average)	2
Yang et al 2014 (52)	20	23-20	Non
Kokot et al 2014 (47)	22	16-28 (average 21.8)	2
Kokot et al 2013 (46)	45	15-28 (average 21.4)	8
Loghmani et al 2013 (48)	41	12-24	3
Chen et al 2010 (43)	24	8-12	Non
You et al 2013 (53)	11	10-12	Non
Alves et al 2012 (30)	47	21-26.4, (average 24.4)	7
Vinh et al 2009 (37)	103	Average 21	4

Chiu et al 2010 (17)	20	18-21	Non
Chiu et al 2009 (18)	18	Average 20	1
Pallua et al 1997 (26)	8	20-30	Non
Telang et al 2009 (50)	9	8-6	2
Rashid et al 2006 (49)	27	18-24	Non
Balakrishnan et al 2012 (4)	16	20-35	1
Epps et al 2011 (45)	10	7-20	Non
Pallua et al 2008 (27)	18	12-20	2
Vinh et al 2007 (60)	32	11-24	3
Di Benedetto et al 2005 (29)	26	12-35	2
Pallua et al 2005 (28)	16	14-30	Non
Pallua et al 2000 (19)	29	Average 22	Non

As with any studies, there will always be limitations. The limitation in this part of the study was about the number of the flaps, and in particular the number of modification procedures performed for the flaps. The modification procedures such as the delay and the expansion were small in number and their effect on the distal flap vascularity could not be assessed accurately, and analyzed statistically without bias. Therefore, in the future, a study with a larger sample size is recommended to achieve more reliable clinical and unbiased statistical results for modification procedures in terms of their effect on the survival length of the supraclavicular flap.

Chapter

6

Conclusion

6. Conclusion

ICG angiogram precisely shows the site of the perforators and superficial course of the artery in the real time of the test. Although CTA performed better in the mapping of the supraclavicular artery, but it has irradiation and the risk of contrast problems.

The distal survival of the supraclavicular artery perforator flap is reliable below 22 cm, but the flaps above that size will increase the risk of distal necrosis.

Chapter

7

Appendix

7. Appendix:

7.1. statistical analysis of the data of Part 1 of the project

7.1.1. statistical analysis of Identification of the Site of the Main Perforator:

Case Processing Summary

	Cases					
	Valid		Missing		Total	
	N	Percent	N	Percent	N	Percent
MODALITY * PERF.SITE	113	100.0%	0	0.0%	113	100.0%

MODALITY * Identification of Site of Perforator Crosstabulation

			IDE_SITE		Total
			No	yes	
MODALITY	1	Count	5	20	25
		% within MODALITY	20.0%	80.0%	100.0%

		Adjusted Residual	-4.1	4.1	
	2	Count	8	9	17
		% within MODALITY	47.1%	52.9%	100.0%
		Adjusted Residual	-.8	.8	
	3	Count	8	12	20
		% within MODALITY	40.0%	60.0%	100.0%
		Adjusted Residual	-1.6	1.6	
	4	Count	20	0	20
		% within MODALITY	100.0%	0.0%	100.0%
		Adjusted Residual	4.4	-4.4	
	5	Count	16	0	16
		% within MODALITY	100.0%	0.0%	100.0%
		Adjusted Residual	3.8	-3.8	
	6	Count	6	9	15

	% within MODALITY	40.0%	60.0%	100.0%
	Adjusted Residual	-1.3	1.3	
Total	Count	63	50	113
	% within MODALITY	55.8%	44.2%	100.0%

Chi-Square Tests

	Value	df	Asymptotic Significance (2-sided)
Pearson Chi-Square	45.566[a]	5	.000
Likelihood Ratio	59.513	5	.000
Linear-by-Linear Association	15.240	1	.000
N of Valid Cases	113		

a. 0 cells (0.0%) have expected count less than 5. The minimum expected count is 6.64.

7.1.2. Statistical analysis of Identification of the course of the artery by 6 different imaging modality

Case Processing Summary

	Cases					
	Valid		Missing		Total	
	N	Percent	N	Percent	N	Percent
MODALITY * COURSE. OF ARTERY	113	100.0%	0	0.0%	113	100.0%

MODALITY * Identification of the Course of the Artery Crosstabulation

			IDE_COURSE			
			Complete	Partial	No	Total
MODALITY	1	Count	0	0	25	25
		% within MODALITY	0.0%	0.0%	100.0%	100.0%
		Adjusted Residual	-1.7	-3.9	4.6	
	2	Count	0	11	6	17

		% within MODALITY	0.0%	64.7%	35.3%	100.0%
		Adjusted Residual	-1.3	3.2	-2.3	
	3	Count	9	6	5	20
		% within MODALITY	45.0%	30.0%	25.0%	100.0%
		Adjusted Residual	6.7	-.2	-3.5	
	4	Count	0	0	20	20
		% within MODALITY	0.0%	0.0%	100.0%	100.0%
		Adjusted Residual	-1.5	-3.4	4.0	
	5	Count	0	10	6	16
		% within MODALITY	0.0%	62.5%	37.5%	100.0%
		Adjusted Residual	-1.3	2.8	-2.0	
	6	Count	0	9	6	15
		% within MODALITY	0.0%	60.0%	40.0%	100.0%
		Adjusted Residual	-1.2	2.5	-1.7	

Total	Count	9	36	68	113
	% within MODALITY	8.0%	31.9%	60.2%	100.0%

Chi-Square Tests

	Value	df	Asymptotic Significance (2-sided)
Pearson Chi-Square	90.512[a]	10	.000
Likelihood Ratio	90.855	10	.000
Linear-by-Linear Association	3.469	1	.063
N of Valid Cases	113		

a. 7 cells (38.9%) have expected count less than 5. The minimum expected count is 1.19.

7.1.3. Statistical analysis of Identification of Mapping of the artery by 6 different imaging modality

Case Processing Summary

	Cases					
	Valid		Missing		Total	
	N	Percent	N	Percent	N	Percent
MODALITY * MAPPING	113	100.0%	0	0.0%	113	100.0%

MODALITY * Mapping of the Artery Crosstabulation

			MAPPING			Total
			Complete	Partial	No	
MODALITY	1	Count	0	0	25	25
		% within MODALITY	0.0%	0.0%	100.0%	100.0%
		Adjusted Residual	-1.7	-2.2	2.9	
	2	Count	0	0	17	17
		% within MODALITY	0.0%	0.0%	100.0%	100.0%
		Adjusted Residual	-1.3	-1.8	2.3	

	3	Count	9	6	5	20
		% within MODALITY	45.0%	30.0%	25.0%	100.0%
		Adjusted Residual	6.7	2.4	-6.5	
	4	Count	0	0	20	20
		% within MODALITY	0.0%	0.0%	100.0%	100.0%
		Adjusted Residual	-1.5	-1.9	2.6	
	5	Count	0	0	16	16
		% within MODALITY	0.0%	0.0%	100.0%	100.0%
		Adjusted Residual	-1.3	-1.7	2.2	
	6	Count	0	9	6	15
		% within MODALITY	0.0%	60.0%	40.0%	100.0%
		Adjusted Residual	-1.2	5.7	-3.9	
Total		Count	9	15	89	113
		% within MODALITY	8.0%	13.3%	78.8%	100.0%

Chi-Square Tests

	Value	df	Asymptotic Significance (2-sided)
Pearson Chi-Square	95.758[a]	10	.000
Likelihood Ratio	85.747	10	.000
Linear-by-Linear Association	2.746	1	.098
N of Valid Cases	113		

a. 12 cells (66.7%) have expected count less than 5. The minimum expected count is 1.19.

7.2. Statistical analysis of the correlations between flap length and necrosis:

Correlations		length	Necrosis
Length	Pearson Correlation	1	.553*
	Sig. (1-tailed)		.039
	N	11	11
Necrosis	Pearson Correlation	.553*	1
	Sig. (1-tailed)	.039	
	N	11	11

Correlation is significant at the 0.05 level (1-tailed).

Bibliography

8. Bibliography

1. Neligan PC, Warren RJ. Plastic Surgery-Aesthetic: Elsevier Health Sciences; 2012.
2. Thorne CH. Grabb and Smith's plastic surgery: Lippincott Williams & Wilkins; 2013.
3. Achauer BM. Burn reconstruction: Thieme Medical Pub; 1991.
4. Balakrishnan T, Sivarajan N. Anatomical study of supraclavicular perforator artery and its clinical application as sensate supraclavicular artery propeller flap in the reconstruction of post burns scar contracture neck. Indian Journal of Science and Technology. 2012;5(8):3137-41.
5. Richards A, Dafydd H. Key notes on plastic surgery: John Wiley & Sons; 2014.
6. Aoyagi F, Fujino T, Ohshiro T. Detection of small vessels for microsurgery by a Doppler flowmeter. Plastic and reconstructive surgery. 1975;55(3):372-3.
7. Smit JM, Klein S, Werker PM. An overview of methods for vascular mapping in the planning of free flaps. Journal of Plastic, Reconstructive & Aesthetic Surgery. 2010;63(9):e674-e82.
8. Gerlock Jr AJ, Perry PE, Goncharenko V, Franklin JD. Evaluation of the Dorsalis Pedis Free Flap Donor Site by Angiography 1. Radiology. 1979;130(2):341-3.
9. May Jr JW, Athanasoulis CA, Donelan MB. Preoperative magnification angiography of donor and recipient sites for clinical free transfer of flaps or digits. Plastic and reconstructive surgery. 1979;64(4):483-90.
10. Hutchinson D. Color duplex imaging. Applications to upper-extremity and microvascular surgery. Hand clinics. 1993;9(1):47-57.
11. Masia J, Clavero J, Larranaga J, Alomar X, Pons G, Serret P. Multidetector-row computed tomography in the planning of abdominal perforator flaps. Journal of Plastic, Reconstructive & Aesthetic Surgery. 2006;59(6):594-9.
12. Fukaya E, Grossman RF, Saloner D, Leon P, Nozaki M, Mathes SJ. Magnetic resonance angiography for free fibula flap transfer. Journal of reconstructive microsurgery. 2007;23(04):205-11.
13. Smit JM, Dimopoulou A, Liss AG, Zeebregts CJ, Kildal M, Whitaker IS, et al. Preoperative CT angiography reduces surgery time in perforator flap reconstruction. Journal of Plastic, Reconstructive & Aesthetic Surgery. 2009;62(9):1112-7.
14. Matsui A, Lee BT, Winer JH, Kianzad V, Frangioni JV. Image-guided perforator flap design using invisible near-infrared light and validation with x-ray angiography. Annals of plastic surgery. 2009;63(3):327.
15. Su W, Lu L, Lazzeri D, Zhang YX, Wang D, Innocenti M, et al. Contrast-enhanced ultrasound combined with three-dimensional reconstruction in preoperative perforator flap planning. Plastic and reconstructive surgery. 2013;131(1):80-93.
16. Sands TT, Martin JB, Simms E, Henderson MM, Friedlander PL, Chiu ES. Supraclavicular artery island flap innervation: anatomical studies and clinical implications. Journal of Plastic, Reconstructive & Aesthetic Surgery. 2012;65(1):68-71.
17. Chiu ES, Liu PH, Baratelli R, Lee MY, Chaffin AE, Friedlander PL. Circumferential pharyngoesophageal reconstruction with a supraclavicular artery island flap. Plastic and reconstructive surgery. 2010;125(1):161-6.
18. Chiu ES, Liu PH, Friedlander PL. Supraclavicular artery island flap for head and neck oncologic reconstruction: indications, complications, and outcomes. Plastic and reconstructive surgery. 2009;124(1):115-23.

19. Pallua N, Noah EM. The tunneled supraclavicular island flap: an optimized technique for head and neck reconstruction. Plastic and reconstructive surgery. 2000;105(3):842-51.
20. Wood-Smith D, Porowski PC. Nursing care of the plastic surgery patient: C. V. Mosby Co.; 1967.
21. Marck KW. A history of noma, the" Face of Poverty". Plastic and reconstructive surgery. 2003;111(5):1702-7.
22. Tellioğlu A. Noma: the Sokoto approach (Eur J Plast Surg [1998] 21: 277). European Journal of Plastic Surgery. 1999;22(2):144-.
23. Hartman EH, Van Damme PA, Sauter H, Suominen SH. The use of the pedicled supraclavicular flap in noma reconstructive surgery. Journal of plastic, reconstructive & aesthetic surgery. 2006;59(4):337-42.
24. Lamberty B, Cormack G. Misconceptions regarding the cervico-humeral flap. British journal of plastic surgery. 1983;36(1):60-3.
25. Chan JW, Wong C, Ward K, Saint-Cyr M, Chiu ES. Three-and four-dimensional computed tomographic angiography studies of the supraclavicular artery island flap. Plastic and reconstructive surgery. 2010;125(2):525-31.
26. Pallua N, Machens H-G, Rennekampff O, Becker M, Berger A. The fasciocutaneous supraclavicular artery island flap for releasing postburn mentosternal contractures. Plastic and reconstructive surgery. 1997;99(7):1878-84.
27. Pallua N, Demir E. Postburn head and neck reconstruction in children with the fasciocutaneous supraclavicular artery island flap. Annals of plastic surgery. 2008;60(3):276-82.
28. Pallua N, Von Heimburg D. Pre-expanded ultra-thin supraclavicular flaps for (full-) face reconstruction with reduced donor-site morbidity and without the need for microsurgery. Plastic and reconstructive surgery. 2005;115(7):1837-44.
29. Di Benedetto G, Aquinati A, Pierangeli M, Scalise A, Bertani A. From the “charretera” to the supraclavicular fascial island flap: Revisitation and further evolution of a controversial flap. Plastic and reconstructive surgery. 2005;115(1):70-6.
30. Alves HR, Ishida LC, Ishida LH, Besteiro JM, Gemperli R, Faria JC, et al. A clinical experience of the supraclavicular flap used to reconstruct head and neck defects in late-stage cancer patients. Journal of Plastic, Reconstructive & Aesthetic Surgery. 2012;65(10):1350-6.
31. Kadakia S, Agarwal J, Mourad M, Ashai S, Lee T, Ducic Y. Supraclavicular Flap Reconstruction of Cutaneous Defects Has Lower Complication Rate than Mucosal Defects. Journal of reconstructive microsurgery. 2017;33(04):275-80.
32. Razdan SN, Albornoz CR, Ro T, Cordeiro PG, Disa JJ, McCarthy CM, et al. Safety of the supraclavicular artery island flap in the setting of neck dissection and radiation therapy. Journal of reconstructive microsurgery. 2015;31(05):378-83.
33. Vinh VQ, Ogawa R, Iwakiri I, Hyakusoku H, Tanuma K. Clinical and anatomical study of cervicopectoral superthin flaps. Plastic and reconstructive surgery. 2007;119(5):1464-71.
34. Wirtz NE, Khariwala SS. Update on the supraclavicular flap. Curr Opin Otolaryngol Head Neck Surg. 2017;25(5):439-44.
35. Pallua N, Wolter TP. Moving forwards: the anterior supraclavicular artery perforator (a-SAP) flap: a new pedicled or free perforator flap based on the anterior supraclavicular vessels. Journal of Plastic, Reconstructive & Aesthetic Surgery. 2013;66(4):489-96.
36. Tayfur V, Magden O, Edizer M, Menderes A. Supraclavicular artery flap. Journal of Craniofacial Surgery. 2010;21(6):1938-40.
37. Vinh VQ, Van Anh T, Ogawa R, Hyakusoku H. Anatomical and clinical studies of the supraclavicular flap: analysis of 103 flaps used to reconstruct neck scar contractures. Plastic and reconstructive surgery. 2009;123(5):1471-80.

38. Margulis A, Agam K, Icekson M, Dotan L, Yanko-Arzi R, Neuman R. The expanded supraclavicular flap, prefabricated with thoracoacromial vessels, for reconstruction of postburn anterior cervical contractures. Plastic and reconstructive surgery. 2007;119(7):2072-7.
39. Heitland AS, Pallua N. The single and double-folded supraclavicular island flap as a new therapy option in the treatment of large facial defects in noma patients. Plastic and reconstructive surgery. 2005;115(6):1591-6.
40. Ismail H, Elshobaky A. Supraclavicular artery perforator flap in management of post-burn neck reconstruction: clinical experience. Annals of burns and fire disasters. 2016;29(3):209.
41. Ortiz CL, Carrasco AV, Torres AN, Sempere LN, Mendoza MM. Supraclavicular bilobed fasciocutaneous flap for postburn cervical contractures. Burns. 2007;33(6):770-5.
42. Chen B, Song H, Xu M, Gao Q. Reconstruction of cica-contracture on the face and neck with skin flap and expanded skin flap pedicled by anterior branch of transverse cervical artery. Journal of Cranio-Maxillofacial Surgery. 2016;44(9):1280-6.
43. Chen W-L, Zhang D-m, Yang Z-h, Huang Z-q, Wang J-g, Zhang B, et al. Extended supraclavicular fasciocutaneous island flap based on the transverse cervical artery for head and neck reconstruction after cancer ablation. Journal of Oral and Maxillofacial Surgery. 2010;68(10):2422-30.
44. Emerick KS, Herr MW, Lin DT, Santos F, Deschler DG. Supraclavicular artery island flap for reconstruction of complex parotidectomy, lateral skull base, and total auriculectomy defects. JAMA Otolaryngology–Head & Neck Surgery. 2014;140(9):861-6.
45. Epps MT, Cannon CL, Wright MJ, Chaffin AE, Newsome RE, Friedlander PL, et al. Aesthetic restoration of parotidectomy contour deformity using the supraclavicular artery island flap. Plastic and reconstructive surgery. 2011;127(5):1925-31.
46. Kokot N, Mazhar K, Reder LS, Peng GL, Sinha UK. The supraclavicular artery island flap in head and neck reconstruction: applications and limitations. JAMA Otolaryngology–Head & Neck Surgery. 2013;139(11):1247-55.
47. Kokot N, Mazhar K, Reder LS, Peng GL, Sinha UK. Use of the supraclavicular artery island flap for reconstruction of cervicofacial defects. Otolaryngology--Head and Neck Surgery. 2014;150(2):222-8.
48. Loghmani S, Eidy M, Mohammadzadeh M, Loghmani A, Raigan F. The supraclavicular flap for reconstruction of post-burn mentosternal contractures. Iranian Red Crescent Medical Journal. 2013;15(4):292.
49. Rashid M, Zia-ul-Islam M, Bhatti AM. The 'expansile'supraclavicular artery flap for release of post-burn neck contractures. Journal of Plastic, Reconstructive & Aesthetic Surgery. 2006;59(10):1094-101.
50. Telang P, Jagannathan M, Devale M. A study of the use of the supraclavicular artery flap for resurfacing of head, neck, and upper torso defects. Indian Journal of Plastic Surgery. 2009;42(1):4.
51. Yang Y, Ren J, Pang X, Bai Y, Yuan W, Xu W. Reconstruction of facial and cervical scar with the expanded supraclavicular island flaps. Zhonghua zheng xing wai ke za zhi= Zhonghua zhengxing waike zazhi= Chinese journal of plastic surgery. 2015;31(1):11-3.
52. Yang Z, Hu C, Li Y, Tang Y, Zhao M, Chen W, et al. Pre-expanded cervico-acromial fasciocutaneous flap based on the supraclavicular artery for resurfacing post-burn neck scar contractures. Annals of plastic surgery. 2014;73:S92-S8.
53. You Y-h, Chen W-l, Zhang D-m. Closure of large oropharyngocutaneous fistulas using a folded extensive supraclavicular fasciocutaneous island flap. Journal of Oral and Maxillofacial Surgery, Medicine, and Pathology. 2013;25(4):310-3.

54. Zhang B, Yan D, Zhang Y, Zhang X, Wan H. Clinical experience with the supraclavicular flap to reconstruct head and neck defects. Zhonghua er bi yan hou tou jing wai ke za zhi= Chinese journal of otorhinolaryngology head and neck surgery. 2015;50(6):468-72.
55. Lamberty B. The supra-clavicular axial patterned flap. British journal of plastic surgery. 1979;32(3):207-12.
56. Mizerny BR, Lessard M-L, Black MJ. Transverse cervical artery fasciocutaneous free flap for head and neck reconstruction: Initial anatomic and dye studies. Otolaryngology-Head and Neck Surgery. 1995;113(5):564-8.
57. ABE M, MURAKAMI G, ABE S, SAKAKURA Y, YAJIMA T. Supraclavicular artery in Japanese: An anatomical basis for the flap using a pedicle containing a cervical, non-perforating cutaneous branch of the superficial cervical artery. Okajimas folia anatomica Japonica. 2000;77(5):149-54.
58. Cordova A, Pirrello R, D'Arpa S, Jeschke J, Brenner E, Moschella F. Vascular anatomy of the supraclavicular area revisited: Feasibility of the free supraclavicular perforator flap. Plastic and reconstructive surgery. 2008;122(5):1399-409.
59. Ma X, Zheng Y, Xia W, Fan X, Li Y, Guo S, et al. An anatomical study with clinical application of one branch of the supraclavicular artery. Clinical Anatomy. 2009;22(2):215-20.
60. Vinh VQ, Ogawa R, Van Anh T, Hyakusoku H. Reconstruction of neck scar contractures using supraclavicular flaps: Retrospective study of 30 cases. Plastic and reconstructive surgery. 2007;119(1):130-5.
61. Gray H. Anatomy of the human body: Lea & Febiger; 1918.
62. Khan UD, Miller J. Reliability of Handheld Doppler in Planning Local Perforator–Based Flaps for Extremities. Aesthetic plastic surgery. 2007;31(5):521-5.
63. Yu P, Youssef A. Efficacy of the handheld Doppler in preoperative identification of the cutaneous perforators in the anterolateral thigh flap. Plastic and reconstructive surgery. 2006;118(4):928-33.
64. Mun G-H, Jeon B-J. An efficient method to increase specificity of acoustic Doppler sonography for planning a perforator flap: perforator compression test. Plastic and reconstructive surgery. 2006;118(1):296-7.
65. Alonso-Burgos A, García-Tutor E, Bastarrika G, Benito A, Domínguez PD, Zubieta JL. Preoperative planning of DIEP and SGAP flaps: preliminary experience with magnetic resonance angiography using 3-tesla equipment and blood-pool contrast medium. Journal of Plastic, Reconstructive & Aesthetic Surgery. 2010;63(2):298-304.
66. Ogawa R, Murakami M, Vinh VQ, Hyakusoku H. Clinical and anatomical study of superficial cervical artery flaps: Retrospective study of reconstructions with 41 flaps and the feasibility of harvesting them as perforator flaps. Plastic and reconstructive surgery. 2006;118(1):95-101.
67. Rozen WM, Garcia-Tutor E, Alonso-Burgos A, Acosta R, Stillaert F, Zubieta JL, et al. Planning and optimising DIEP flaps with virtual surgery: the Navarra experience. Journal of Plastic, Reconstructive & Aesthetic Surgery. 2010;63(2):289-97.
68. Mathes DW, Neligan PC. Current techniques in preoperative imaging for abdomen-based perforator flap microsurgical breast reconstruction. Journal of reconstructive microsurgery. 2010;26(01):003-10.
69. Pacifico M, See M, Cavale N, Collyer J, Francis I, Jones M, et al. Preoperative planning for DIEP breast reconstruction: early experience of the use of computerised tomography angiography with VoNavix 3D software for perforator navigation. Journal of Plastic, Reconstructive & Aesthetic Surgery. 2009;62(11):1464-9.

70. Rozen W, Ashton M, Grinsell D, Stella D, Phillips T, Taylor G. Establishing the case for CT angiography in the preoperative imaging of abdominal wall perforators. Microsurgery. 2008;28(5):306-13.
71. Rozen WM, Ashton M. The "limited rectus sheath incisions" technique for DIEP flaps using preoperative CT angiography. Microsurgery. 2009;29(7):525-8.
72. Ribuffo D, Atzeni M, Saba L, Milia A, Guerra M, Mallarini G. Angio computed tomography preoperative evaluation for anterolateral thigh flap harvesting. Annals of plastic surgery. 2009;62(4):368-71.
73. Kazanjian V, Converse JM. The surgical treatment of facial injuries, ed. 2, Baltimore, 1959. Williams & Wilkins Company.
74. Rozen WM, Phillips TJ, Ashton MW, Stella DL, Gibson RN, Taylor GI. Preoperative imaging for DIEA perforator flaps: a comparative study of computed tomographic angiography and Doppler ultrasound. Plastic and reconstructive surgery. 2008;121(1):9-16.
75. Singh J, Daftary A. Iodinated contrast media and their adverse reactions. Journal of nuclear medicine technology. 2008;36(2):69-74.
76. Chernyak V, Rozenblit AM, Greenspun DT, Levine JL, Milikow DL, Chia FA, et al. Breast reconstruction with deep inferior epigastric artery perforator flap: 3.0-T gadolinium-enhanced MR imaging for preoperative localization of abdominal wall perforators. Radiology. 2009;250(2):417-24.
77. Rozen WM, Stella DL, Phillips TJ, Ashton MW, Corlett RJ, Taylor GI. Magnetic resonance angiography in the preoperative planning of DIEA perforator flaps. Plastic and reconstructive surgery. 2008;122(6):222e-3e.
78. Kelly AM, Cronin P, Hussain HK, Londy FJ, Chepeha DB, Carlos RC. Preoperative MR angiography in free fibula flap transfer for head and neck cancer: clinical application and influence on surgical decision making. American Journal of Roentgenology. 2007;188(1):268-74.
79. Lohan DG, Tomasian A, Krishnam M, Jonnala P, Blackwell KE, Finn JP. MR angiography of lower extremities at 3 T: presurgical planning of fibular free flap transfer for facial reconstruction. American Journal of Roentgenology. 2008;190(3):770-6.
80. Seres L, Csaszar J, Voros E, Borbely L. Donor site angiography before mandibular reconstruction with fibula free flap. Journal of Craniofacial Surgery. 2001;12(6):608-13.
81. Tan O, Kantarci M, Parmaksizoglu D, Uyanik U, Durur I. Determination of the recipient vessels in the head and neck using multislice spiral computed tomography angiography before free flap surgery: a preliminary study. Journal of Craniofacial Surgery. 2007;18(6):1284-9.
82. Herz D, DaJusta D, Ching C, McLeod D. Segmental arterial mapping during pediatric robot-assisted laparoscopic heminephrectomy: A descriptive series. Journal of pediatric urology. 2016;12(4):266. e1-. e6.
83. Namikawa T, Sato T, Hanazaki K. Recent advances in near-infrared fluorescence-guided imaging surgery using indocyanine green. Surgery today. 2015;45(12):1467-74.